



# Deciphering linkages between DON and the microbial community for nitrogen removal using two green sorption media in a surface water filtration system

Jinxiang Cheng<sup>a</sup>, Alejandra Robles-Lecompte<sup>a</sup>, Amy M. McKenna<sup>b,c</sup>, Ni-Bin Chang<sup>a,\*</sup>

<sup>a</sup> Department of Civil, Environmental, and Construction Engineering, University of Central Florida, Orlando, FL, USA

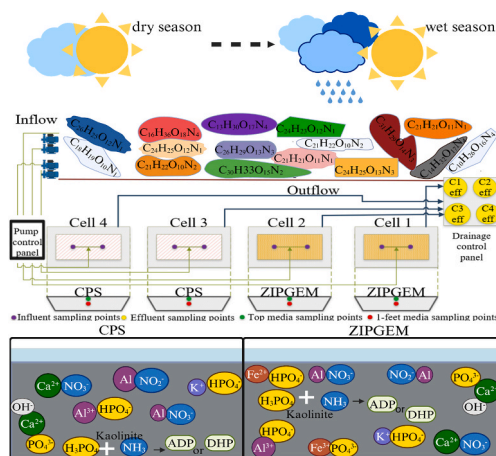
<sup>b</sup> National High Magnetic Field Laboratory, Florida State University, Tallahassee, FL, USA

<sup>c</sup> Department of Soil and Crop Sciences, Colorado State University, Fort Collins, CO, USA

## HIGHLIGHTS

- ZIPGEM media mix performs better than CPS media mix for nitrogen removal.
- DON decomposition deeply affects the removal rate of nitrogen in the surface water filtration system.
- Photoammonification and mineralization are the key steps of the DON partial fraction decomposition.

## GRAPHICAL ABSTRACT



## ARTICLE INFO

Handling editor: Y Yeomin Yoon

### Keywords:

Specialty adsorbent  
Filtration  
Microbial ecology  
Dissolved organic nitrogen  
Denitrification

## ABSTRACT

The presence of dissolved organic nitrogen (DON) in stormwater treatment processes is a continuous challenge because of the intertwined nature of its decomposition, bioavailability, and biodegradability and its unclear molecular characteristics. In this paper, 21 T Fourier transform ion cyclotron resonance mass spectrometry (FT-ICR MS) in combination with quantitative polymerase chain reaction was applied to elucidate the molecular change of DON and microbial population dynamics in a field-scale water filtration system filled with two specialty adsorbents for comparison in South Florida where the dry and wet seasons are distinctive annually. The adsorbents included CPS (clay-perlite and sand sorption media) and ZIPGEM (zero-valent iron and perlite-based green environmental media). Our study revealed that seasonal effects can significantly influence the dynamic characteristics and biodegradability of DON. The microbial population density in the filter beds indicated that three microbial species in the nitrogen cycle were particularly thrived for denitrification, dissimilatory nitrate

\* Corresponding author.

E-mail address: [nchang@ucf.edu](mailto:nchang@ucf.edu) (N.-B. Chang).

<https://doi.org/10.1016/j.chemosphere.2024.142042>

Received 23 February 2024; Received in revised form 11 April 2024; Accepted 12 April 2024

Available online 13 April 2024

0045-6535/© 2024 The Authors. Published by Elsevier Ltd. This is an open access article under the CC BY license (<http://creativecommons.org/licenses/by/4.0/>).

reduction to ammonium, and anaerobic ammonium oxidation via competition and commensalism relationships during the wet season. Also, there was a decrease in the compositional complexity and molecular weight of the DON groups ( $C_nH_mO_pN_1$ ,  $C_nH_mO_pN_2$ ,  $C_nH_mO_pN_3$ , and  $C_nH_mO_pN_4$ ), revealed by the 21 T FT-ICR MS bioassay, driven by a microbial population quantified by polymerase chain reaction from the dry to the wet season. These findings indirectly corroborate the assumption that the metabolism of microorganisms is much more vigorous in the wet season. The results affirm that the sustainable materials (CPS and ZIPGEM) can sustain nitrogen removal intermittently by providing a suitable living environment in which the metabolism of microbial species can be cultivated and enhanced to facilitate physico-chemical nitrogen removal across the two types of green sorption media.

## 1. Introduction

Dissolved organic nitrogen (DON) is an important component of the dissolved nitrogen pool in stormwater that contributes to the eutrophication of surface water. DON can affect stormwater quality via a complex fate and transport process of organic pollutants (Akkanen and Kukkonen, 2003) partially driven by microbial growth acceleration in the flow field (Berman and Bronk, 2003). DON groups are not inert matters and can be utilized by microbiological processes with sophisticated linkages. The role of DON in primary productivity was recognized as far back as the 1980s (Antia et al., 1991). Moreover, the turnover time of DON and the easy decomposition stage of DON are 21 days and 17 days, respectively (Jackson and Williams, 1985). The DON growth rate for Castle Lake in California was fast in early summer, reaching  $0.31 \mu\text{M N/d}$  (Zehr et al., 1988). It was also found that the decomposition rate of DON in the euphotic zone of Lake Kizaki, Japan, reached 8.6% with a turnover time of about 12 days (Takahashi, 1981). However, the residence time of DON in Lake Kizaki ranged from 1.4 to 21 days, and the corresponding concentrations ranged from 3.5 to  $10.4 \mu\text{mol/L}$  (Haga et al., 2001). In Lake Mendota in Wisconsin, at the surface, the concentration of DON was  $44.7 \mu\text{M N}$ , whereas at 20 m deep, the concentration of DON was  $44.2 \mu\text{M N}$  (Wetzel, 2001), confirming that Lake Mendota is a highly eutrophic lake. In some freshwater ecosystems, the concentration of DON is higher than 50% of total dissolved nitrogen (TDN) and 5–10 times higher than that of particulate organic nitrogen (Wheeler and Kirchman, 1986). Microorganisms directly use 10–70% of DON (Watanabe et al., 2014), confirming that DON and its components can affect water quality. All the above studies have shown that DON is one of the important factors in eutrophication and is constantly being produced and used by microorganisms. DON properties are also affected by different uptake and consumption for growth, energy storage, metabolism, excretion of secondary compounds, and cleavage products (Kujawinski et al., 2004; Stibal et al., 2012; Koch et al., 2014; Dittmar and Stubbins, 2014; H. Xu et al., 2020). The microbial community is shaped to some extent by DON characteristics (Douterelo et al., 2014) that complicate the design of some stormwater treatment processes (Emtiazi et al., 2004). However, the fate of DON in stormwater treatment has not been fully studied. Thus, a better understanding of the interactions and linkages between DON molecular characteristics and diverse microbial communities in stormwater may help predict the fate of DON and optimize the treatment efficiency of stormwater.

Two different bioassay procedures were used to measure DON utilization, including the bioavailable DON (ABDON) approach (algal growth and bacterial growth) (Pehlivanoglu and Sedlak, 2004) and the biodegradable DON (BDON) approach (bacterial growth) (Khan et al., 2009; Osborne et al., 2013; Lusk and Toor, 2016). Previous research has suggested that the bioavailability and biodegradability of DON (ABDON/DON or BDON/DON) are related to the chemical composition of DON. Studies have shown that low molecular weight ( $<1 \text{ kDa}$ ) DON (LMW-DON) can more easily stimulate algal growth, causing a more significant impact on the water environment than high molecular weight ( $>1 \text{ kDa}$ ) DON (HMW-DON) (Eom et al., 2017). Some forms of DON, such as free amino acids, are readily bioavailable for direct algal uptake, whereas some forms are bioavailable after bacterial degradation

(Pehlivanoglu and Sedlak, 2004; Bronk et al., 2007). DON can become more bioavailable to algae through hydrolysis or degradation and mineralization by bacteria (Simsek et al., 2013; Alimoradi et al., 2020). In this study, because of the role of microorganisms in degrading DON (the fraction of DON that can be mineralized by mixed bacteria), the BDON protocol fits better.

We developed a novel field-scale study to compare the performance of nitrogen removal via two specialty adsorbents aiming to link pattern shifts of DON decomposition in relation to microbial species population dynamics in the nitrogen cycle under wet and dry climatic conditions in South Florida. Whereas the former runs from May till September, the latter starts runs from October till April of the next year. The two specialty adsorbents (a.k.a. green sorption media) are CPS (clay-perlite and sand sorption media) and ZIPGEM (zero-valent iron and perlite-based green environmental media). The components of these two green adsorption media, such as sand, ZVI, and perlite, are sustainable because they can be used as raw materials in cementitious and geopolymeric concretes (Dong et al., 2021) or for environmental remediation by increasing the effectiveness and efficiency of purification of soils or groundwaters (Zhang et al., 2022). Therefore, our field-scale study emphasized not only nitrogen removal but also material sustainability.

The objectives of this study are to (1) link DON decomposition and microorganism population dynamics (e.g., AOB, NOB, nirS, nrfA, Anammox, Comammox, and IRB) with microbial ecology implications, (2) evaluate the influence of varying wet and dry climatic conditions on the nitrogen removal from a microbiological perspective, and (3) explore the impact of microbial communities on DON composition and bioavailability under wet and dry climatic conditions. The study aims to address the following research questions: (1) How do the microbial ecology implications differ from ZIPGEM to CPS in terms of nitrification, denitrification, and dissimilatory nitrate reduction to ammonium, anaerobic ammonium oxidation, and complete ammonia oxidation? (2) How can DON composition and concentration as well as the biodegradability of DON be affected by wet and dry climatic conditions? (3) How does seasonal change affect microbial species development in terms of population dynamics, metabolic rate, and cell conditions that in turn affect DON decomposition? We applied negative-ion electrospray ionization 21 T Fourier-transform ion cyclotron resonance mass spectrometry (FT-ICR MS), quantitative polymerase chain reaction (qPCR), and bioassays to answer these questions. Therefore, this study links DON decomposition, ammonification, nitrification, and denitrification processes under the climatic impact to investigate key scientific issues integral to stormwater treatment. To our knowledge, this is the first endeavor to explore the molecular composition and biodegradability of DON in relation to microbial communities based on real-world conditions via a field-scale surface water filtration system with new specialty adsorbents (a.k.a. green sorption media). These green sorption media are sustainable because they are mixed with recycled and natural material.

## 2. The field-scale surface water filtration system with green sorption media

The construction of our field-scale water filtration system

commenced in the early days of September 2022, following the acquisition of the right-of-way permit (site access permit) from the South Florida Water Management District and Army Corps of Engineers. Then a series of steps were taken for site clearance, accurate site surveys, excavation, liner positioning and welding, installation of pumping stations and a piping system, wiring for the control box, wireless communication and data storage, and setting up drainage boxes. The mixing and installation of the two green sorption media (i.e., specialty adsorbents) concluded the construction in January 2023. On January 27, 2023, samples of raw and mixed green sorption media were collected by the UCF research team for material characterization. The team validated the efficacy of media preparation and mixing in the field by generating mixed media gradation curves by utilizing on-site sieve analysis driven by a generator. As of February 17, 2023, the entire construction project had reached completion. Ultimately, four filtration cells (i.e., two for CPS and two for ZIPGEM, Fig. 1a and c) were built, each measuring 6.7 m (22 ft) in width, 13.3 m (43.5 ft) in length, and reaching a maximum depth of 1.2 m (4 ft), aligned with the C-23 canal in Port St. Lucie, located to the east of the primary north-south Interstate Highway (I-95) in South Florida (Fig. 1a).

ZIPGEM media were used to fill cells 1 and 2 at a depth of 0.6 m (2 feet), whereas cells 3 and 4 received CPS media for the same depth. Situated in the South Florida Water Management District, the engineered C-23 canal receives the stormwater runoff from the upstream agricultural field and drains to the St. Lucie estuary and then to the Atlantic Ocean, transporting over 160.1 million tonnes (42.3 billion gallons) of water annually. This location is situated at latitude ( $27^{\circ}12'19.8''N$ ) and longitude ( $80^{\circ}23'47.8''W$ ). Programs for total maximum daily load (TMDL) and the associated basin management action plan have been established at the waterbody identification number tier to diminish nutrient levels in the St. Lucie River Basin. The desired TMDL concentrations are  $0.72 \text{ mg L}^{-1}$  for total nitrogen (TN) and  $0.081 \text{ mg L}^{-1}$  for total phosphorus (TP).

Filled with ZIPGEM and CPS (Fig. 1c), the filtration system uses two green sorption media made up of mixed recycled and natural components including sand, ZVI, and perlite. Opting to repurpose the depleted ZIPGEM and CPS as a soil amendment for local agricultural fields, rather than disposing them once they are fully utilized, offers greater benefits because it simultaneously aids in achieving the United Nations Sustainable Development Goals for enhancing soil quality. The chemical element compositions of the used ZIPGEM and CPS (EV 3 and EV9) are presented in Table S5 and Table S7, respectively; the increasing P percentage in spent media compared to raw media is especially important, varying from 3.76% (raw ZIPGEM) to 4.42% (spent ZIPGEM) in EV3 and then to 4.78% (spent ZIPGEM) in EV9. This observation confirms that the reuse of the spent media as a soil amendment is feasible, because it can lower the cost and environmental impact in a circular economy, thereby reducing the ecological effects of phosphorus mining and maintaining the limited phosphorus resource in the St. Lucie River watershed adjacent to the Indian River Lagoon, which is a nutrient-rich water body.

This study shows that the exploration of interactive connections between DON and microspecies in the nitrogen cycle becomes feasible with an integrated DON characterization and qPCR analysis. Nitrogen mineralization involves transforming organic nitrogen into its inorganic variants through a dual-step process starting with aminization and then proceeding to ammonification. Aminization involves microorganisms decomposing intricate proteins into basic amino acids, amides, and amines (proteins  $\rightarrow$  R-NH<sub>2</sub>, where R is a carbon chain). Ammonification denotes a chemical process in which NH<sub>2</sub> groups transform into ammonia or its ionic variant, ammonium (NH<sub>4</sub><sup>+</sup>). The degree of mineralization and ammonification can be detailed through the examination of DON's concentration, composition, and structure. The process of nitrification involves the oxidation of ammonia or ammonium ions into nitrite (NO<sub>2</sub><sup>-</sup>) by AOB, followed by their conversion to nitrate (NO<sub>3</sub><sup>-</sup>) by NOB. Denitrification refers to the biochemical process in which

microbes transform the nitrate nitrogen (NO<sub>3</sub><sup>-</sup>) into nitrogen gas (N<sub>2</sub>) through a series of intermediate products, specifically nitrite (NO<sub>2</sub><sup>-</sup>), nitric oxide (NO), and nitrogen oxide (N<sub>2</sub>O). In denitrification, the second step involves converting NO<sub>2</sub><sup>-</sup> into NO via nirS, a crucial step that restricts the rate of denitrification. Consequently, examining the populations of AOB, NOB, and nirS can elucidate the degree of nitrification and denitrification processes. The flowchart of this experimental study can be seen in Fig. S1.

### 3. Material and methods

#### 3.1. Sample collection and analysis

From March 1 to July 3, 2023, 10 manual sampling and monitoring events took place at a frequency of approximately every 2 weeks and are summarized in Table S1. Each sampling event included collecting water (influent and effluent, Fig. 1a and b) and media samples from each of the filtration cells (Fig. 1c); manually recording basic water quality parameters; and maintaining *in situ* automated water quality sensors. All field water sampling events were conducted according to the Florida Department of Environmental Protection Standard Operating Procedures (FDEP SOP: FT1000, FS1000, FS2000 and FS2100). Nutrient pollutants were analyzed by Eurofins Environmental Testing Southeast Laboratories (formerly Flowers; Table S2). The collected media sample were stored at  $-80^{\circ}\text{C}$  in the bioenvironmental research laboratory at UCF until gene extraction.

#### 3.2. DON and its biodegradability determination

DON, the N-bearing organic component, was obtained with solid phase extraction (SPE) as described by Dittmar et al. and Stubbins (2014). The concentration of DON was calculated as the difference between TDN and the sum of inorganic nitrogen species (i.e., NH<sub>4</sub><sup>+</sup>, NO<sub>3</sub><sup>-</sup> and NO<sub>2</sub><sup>-</sup>; eq (1)). The concentration of BDON was determined by a 5-day bacterial growth cycle described by Osborne et al. (2013) and Lusk and Toor (2016). The bioassay studies were initiated by mixing 200 mL of effluents and 75 mL of inoculum (canal water) in a conical flask (designated as T<sub>0</sub>) and filtrated through a 0.45 μm filter and refrigerated (4 °C) until analysis. The samples labeled T<sub>0</sub> were analyzed for TN and inorganic nitrogen species (i.e., NH<sub>4</sub><sup>+</sup>, NO<sub>3</sub><sup>-</sup> and NO<sub>2</sub><sup>-</sup>) via Hach kits. Subsequently, the differences between TN and the sum of inorganic nitrogen species (i.e., NH<sub>4</sub><sup>+</sup>, NO<sub>3</sub><sup>-</sup> and NO<sub>2</sub><sup>-</sup>) were cataloged as dissolved organics. The samples in another batch of flasks, labeled T<sub>5</sub>, underwent a 5-day incubation period following a light-and-dark cycle of 12:12. Following a period of 5 days, the samples that had been incubated underwent filtration and were examined by the same way as the T<sub>0</sub> samples. The calculation of DON's biodegradability was based on the variation in DON levels between the T<sub>5</sub> and T<sub>0</sub> samples (eq (2)) (Lusk and Toor, 2016). DON degradability was calculated according to eq (3) (Hu et al., 2016).

$$\text{DON (mg}\cdot\text{L}^{-1}) = \text{TDN} - (\text{Ammonianitrogen} - \text{Nitritenitrogen} - \text{Nitratenitrogen}) \quad (1)$$

$$\text{BDON (mg}\cdot\text{L}^{-1}) = \text{DON}_0 - \text{DON}_5 \quad (2)$$

$$\text{DON degradability (\%)} = \frac{\text{BDON}}{\text{DON}} * 100\% \quad (3)$$

DON<sub>0</sub> and DON<sub>5</sub> are DON before (at T<sub>0</sub>) and after (at T<sub>5</sub>) incubation.

#### 3.3. DON molecular composition

Negative-ion electrospray ionization FT-ICR MS was used to analyze the molecular composition of DON at the National High Magnetic Field Laboratory in Tallahassee, FL. DOM extracts were analyzed with a





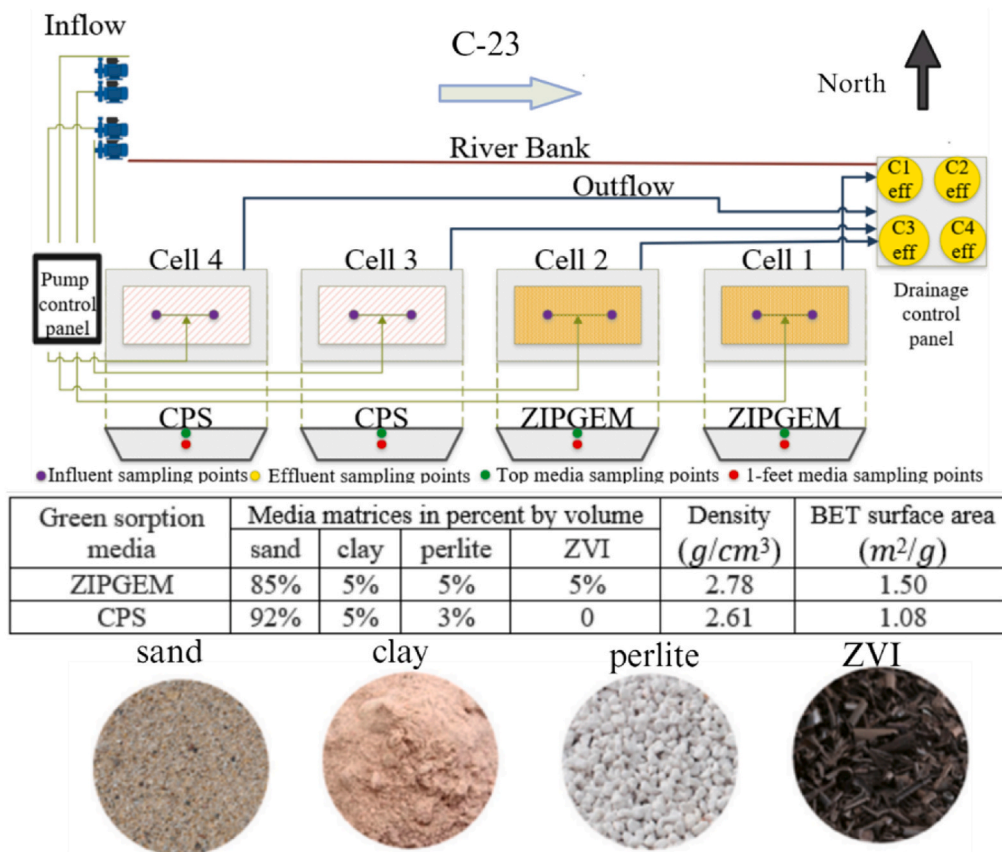


(a)



(b)

 Influent Sample Collection Point  
 Effluent Sample Collection Point



(c)

Fig. 1. (a) Panoramic view of four filter cells with influent and effluent sampling locations; (b) effluent water sampling locations next to the drainage box; (c) sustainable filtration materials and technologies of the surface water filtration system.



custom-built hybrid linear ion trap FT-ICR mass spectrometer equipped with a 21 T superconducting solenoid magnet (Hendrickson et al., 2015; Smith et al., 2018). Peaks with a signal magnitude greater than 6 times the baseline root-mean-square (RMS) noise at  $m/z$  500 were exported to peak lists, and molecular formula assignments and data visualization were performed with PetroOrg software [Corilo, Y.E. PetroOrg Software; Florida State University, Omics: Tallahassee, FL, 2014]. Molecular formula assignments with an error  $>0.5$  parts per million were discarded, and only chemical classes with a combined relative abundance of  $\geq 0.15\%$  of the total were considered. Based on formula assignments, the molecules detected by FT-ICR MS were categorized as lipids (O/C = 0–0.3, H/C = 1.5–2.2), proteins (O/C = 0.3–0.65, H/C = 1.5–2.2, N/C  $\geq 0.05$ ), carbohydrates (O/C = 0.65–1.2, H/C = 1.5–2.2), lignin-like (O/C = 0.1–0.65, H/C = 0.7–1.7), tannin (O/C = 0.65–1.1, H/C = 0.5–1.5), or condensed aromatics (O/C = 0.1–0.65, H/C = 0.1–0.7) and unsaturated hydrocarbons (O/C = 0–0.1 and H/C = 0.7–1.5) (Antony et al., 2014; Feng et al., 2016). For all mass spectra presented herein, 21,894–31,929 peaks were assigned elemental compositions with a root-mean-square mass measurement accuracy of 54–64 ppb, an achieved resolving power of 1,000,000 at  $m/z$  200, and with an achieved resolving power of 2,000,000 at  $m/z$  400. Table S3 shows the number of assignments and RMS errors for all spectra presented herein.

### 3.4. Material characterization

The chemical characterization of these media mixes was further examined to better understand their effects on nitrogen removal mechanisms. XRF elemental composition was performed with the PANalytical Epsilon. XRD spectroscopy was performed with a PANalytical Empyrean X-ray diffraction instrument. FE-SEM spectra were carried out via a Zeiss ULTRA-55 electron microscope operating at an accelerating voltage of 10 kV.

### 3.5. Quantitative PCR analysis

Microbial organisms play an important role in the nitrogen cycle and can provide continual treatment in a nitrogen-polluted water system. We anticipate that the inclusion of biological nitrogen removal coupled with physicochemical adsorption can provide a long-term capacity for total nitrogen removal, which includes removing the nitrogen species of nitrate, nitrite, ammonia, and organic nitrogen. DNA was extracted from

the collected media samples with a DNeasy PowerSoil Kit with PowerBead tubes, Solutions C1 to C5, MB Spin Columns, and 2 mL collection tubes, followed by denaturation, annealing, extension, and DNA amplification. In the media bed of this study, the common microbial species involved in the nitrogen-cycle include anaerobic ammonium oxidation (Anammox) (Snoeyenbos-West et al., 2000; Tsushima et al., 2007), ammonia-oxidizing bacteria (AOB) (Rotthauwe et al., 1997), nitrite-oxidizing bacteria (NOB) (Dionisi et al., 2002), dissimilatory nitrate-reducing bacteria (DNRA) and NADPH-flavin reductase A (nrfA) (Yin et al., 2017), denitrifiers (Azziz et al., 2017), complete ammonia oxidation bacteria (Comammox) (Xia et al., 2018), and iron-reducing bacteria (IRB) (Stults et al., 2001). The microbiological species target gene, primer information, and running method are listed in Table S4.

## 4. Results

### 4.1. Nitrogen removal

Fig. 2 displays a detailed, event-based performance comparison between the two types of green sorption media. In the case of ZIPGEM, the efficiency of TN removal remained under 50% in just three instances: event 6, event 9, and event 10. In the case of CPS, the efficiency of removing TN remained below 50% across 7 sampling instances. In the case of sampling event 9, ZIPGEM and CPS recorded the minimal TN removal percentage, amounting to 15.39% and 3.49% respectively. Nonetheless, ZIPGEM outperformed CPS significantly in the overall elimination of TN (Fig. 2a).

The efficiency of ZIPGEM in removing TKN surpassed that of CPS (Fig. 2b). Additionally, ZIPGEM experienced a single sampling occurrence where the removal efficiency was under 50%, in contrast to CPS, which had two such events with a removal efficiency below 50%. The fifth sampling event showed minimal elimination of TKN in both ZIPGEM and CPS, potentially linked to seasonal variations. Seasonal changes impacted how effectively ZIPGEM and CPS eliminated ammonia. During the first four sampling events, CPS appeared to remove slightly more ammonia than ZIPGEM, but the difference was small. Starting with the fifth occurrence, ZIPGEM and CPS demonstrated reduced effectiveness in ammonia removal (Fig. 2c). Nonetheless, this fails to demonstrate the ineffectiveness of ZIPGEM and CPS in ammonia elimination. The negative figures could stem from the lower ammonia nitrogen levels in influents compared to effluents, owing to the ongoing release of ammonia from photoammonification, bacterial

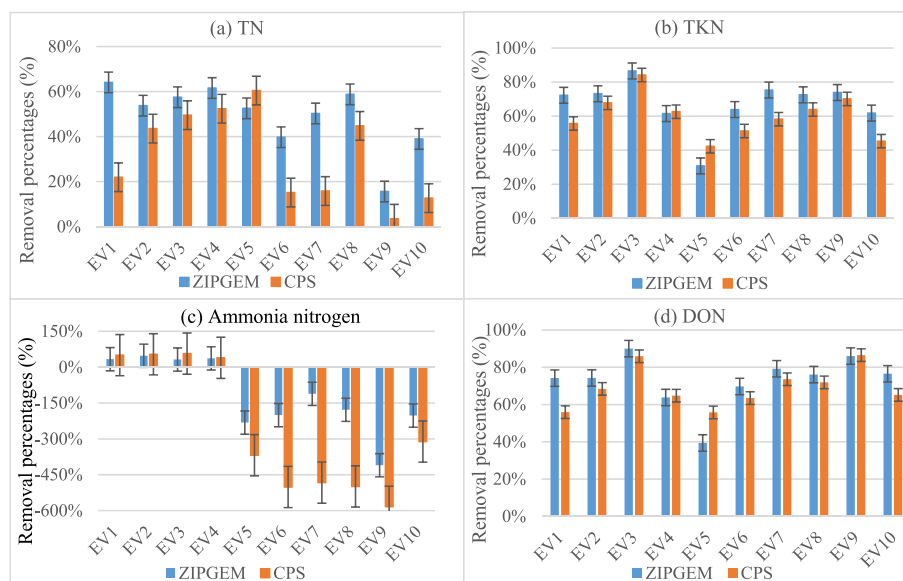


Fig. 2. Removal percentages of (a) TN, (b) TKN, (c) ammonia nitrogen, and (d) DON by ZIPGEM and CPS.

ammonification, and DON mineralization (Davis et al., 2006; Liu et al., 2010; Shrestha et al., 2018). Nonetheless, ZIPGEM seems to exhibit superior adaptability to seasonal changes compared to CPS, because the removal percentage is less negative than CPS in the wet season.

The efficiency of ZIPGEM in removing DON surpassed that of CPS, even though ZIPGEM's DON elimination rate was less than CPS's during event 5 (Fig. 2d). Nonetheless, the rate of removal varied more during the dry season than the wet season. Additionally, ZIPGEM can achieve a 3%–15% greater efficiency in eliminating DON compared to CPS. Compared to CPS, ZIPGEM showed a notably greater efficiency in TP elimination, ranging from 30 to 60% (Fig. S2a). The efficiency of TP elimination using ZIPGEM exceeded 70% and was marginally reduced during the initial sampling occurrence. By contrast, CPS's elimination rate was a mere 60% during the 10th sampling. ZIPGEM's mean TP elimination rate stood at 79.58%, in contrast to CPS's mere 15.49%. During the 10th sampling, ZIPGEM recorded a 96.22% success rate, in contrast to CPS's 61.04% removal percentage. In every sampling instance, ZIPGEM showed a notably greater efficiency (40–60%) in OP elimination than CPS, averaging a removal percentage of 73.16% for ZIPGEM and –134.97% for CPS (Fig. S2b). This phenomenon could stem from the discharge of orthophosphate from basic materials like sand, attributed to the geological formation of sandy soil (Jasinski, 2013) and

widespread farming methods (Duan et al., 2021) in Florida. Even though ZIPGEM outperformed CPS in nutrient removal, both media have an edge over alternative treatment methods according to a cost-benefit analysis. More details can be seen in Table S5.

#### 4.2. Material characterization

Silicon is the most abundant element in the raw ZIPGEM (Table S6). However, in the dry (i.e., when EV3 was selected as representative) and wet (when EV9 was selected as representative) seasons, the proportion of silicon showed a significant decreasing trend from 67.01% in the original to 53.15% in EV3 and again to 42.14% in EV9, in contrast to the increase in the proportion of the metallic elements, for example, calcium, aluminum, and iron, which are the second, third, and fourth most abundant elements in the raw ZIPGEM, with calcium rising from 4.60% in raw to 5.30% in EV3 and again to 6.11% in EV9, aluminum rising from 8.52% in raw to 9.04% in EV3 and again to 15.53% in EV9, and iron also rising from 7.47% in raw to 23.39% in EV3 and again to 25.74% at EV9.

Regarding position, the proportion of elements tends to be higher in the top medium than in the 1-foot samples. This may be because of water flow direction. From Table S7, silica is the most abundant oxide in the

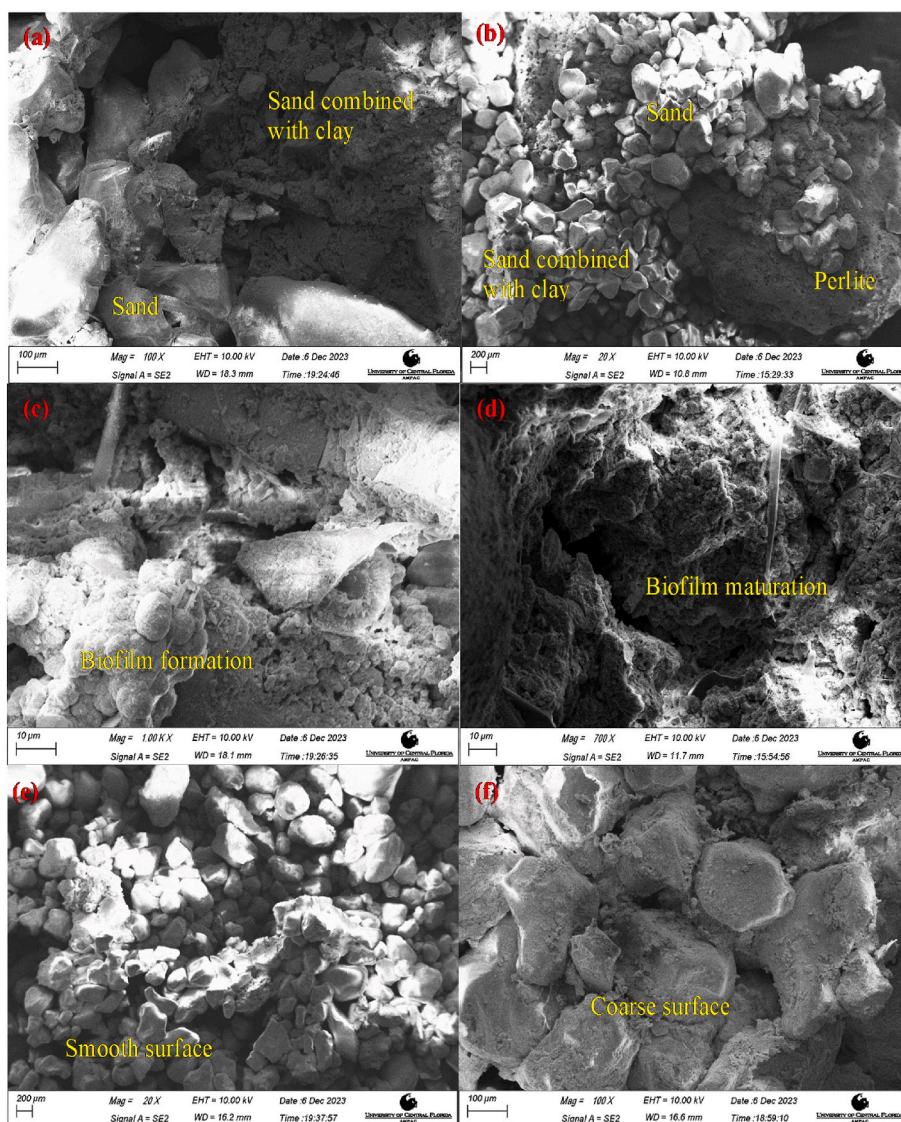


Fig. 3. (a)top, ZIPGEM at EV3(b) top, ZIPGEM at EV9(c) biofilm top, ZIPGEM at EV3 (d) biofilm top, ZIPGEM at EV9(e) 1 foot, ZIPGEM at EV3, (f) 1 foot, ZIPGEM at EV9.



pristine ZIPGEM. However, in both the dry and wet seasons, the proportion of silica showed a significant decreasing trend from 80.11% in the pristine to 55.67% in the EV3, and again to 40.45% in the EV9; in contrast, the proportion of metal oxides rises. For example,  $\text{Al}_2\text{O}_3$  rises from 9.6% to 14.42% in EV3 and again to 17.30% in EV9, while  $\text{Fe}_2\text{O}_3$  also rises from 1.87% to 17.29% in EV3 and again to 27.13% in EV9. CaO also rises from 2.32% to 4.53% in EV3 and again to 5.13% in EV9. Tables S8 and S9 summarize more details for CPS, confirming a similar trend in chemical element composition changes to ZIPGEM from the dry to the wet season.

Additionally, the FE-SEM image (Fig. 3) reveals that during the dry season, biofilm remains in an out-of-growth stage, whereas in the wet season, it reaches maturity, particularly in its three-dimensional and stratified forms. The development of biofilms is intimately linked to the creation and application of DON molecules. Likewise, a comparison of the medium's surface reveals that it maintains a comparatively smooth appearance during the dry season. Conversely, the surface in the wet season exhibits a rougher texture, indicating a heightened intensity of intermolecular activity. According to Fig. S3,  $\text{SiO}_2$  and  $\text{O}_2\text{Si}_1$  are the first two main compounds in ZIPGEM and CPS. However, for ZIPGEM,  $\text{FePO}_4 \cdot 2\text{H}_2\text{O}$  is the third main compound, which demonstrates that  $\text{Fe}^{3+}$  from ZVI is plentiful enough to form various forms of Fe oxides with other elements to remove nutrients.

Notably, the P composition in Table S6 and Table S8, and the  $\text{P}_2\text{O}_5$  composition in Tables S7 and S9, demonstrate that from the dry to the wet season, both ZIPGEM and CPS experienced a higher percentage of P and  $\text{P}_2\text{O}_5$  composition in the spent media than in the raw media. This indicates the potential of spent media for reuse as a soil amendment to enhance the supply of phosphorus for crops.

#### 4.3. DON composition changes

Based on the number of N atoms in the DON molecule,  $\text{C}_n\text{H}_m\text{O}_p\text{N}_1$ ,  $\text{C}_n\text{H}_m\text{O}_p\text{N}_2$ ,  $\text{C}_n\text{H}_m\text{O}_p\text{N}_3$ , and  $\text{C}_n\text{H}_m\text{O}_p\text{N}_4$  indicated one, two, three, and four N atoms in the DON molecule, respectively. Basically, the molecular weight and the complexity of the compound structure of DON in the CPS-filled cell effluents were higher than that of the ZIPGEM-filled cell effluents. For example, in the effluents of cell 3 at EV9 (Fig. 4), the species with the highest relative abundance in  $\text{C}_n\text{H}_m\text{O}_p\text{N}_1$  and  $\text{C}_n\text{H}_m\text{O}_p\text{N}_2$  were  $\text{C}_{21}\text{H}_{21}\text{O}_{11}\text{N}_1$  (462.1 Da) and  $\text{C}_{21}\text{H}_{22}\text{O}_{11}\text{N}_2$  (477.12 Da) respectively, whereas  $\text{C}_{18}\text{H}_{19}\text{O}_{10}\text{N}_1$  (408.09 Da) and  $\text{C}_{20}\text{H}_{22}\text{O}_{10}\text{N}_2$  (449.12 Da) were the two species in the corresponding class of cell 1. The same applies to the dry season. This also indicates that the intensity of the bacterial metabolism in ZIPGEM is more robust than that in CPS. Even though more DON is required for the more vital bacterial metabolism in ZIPGEM, at the same time, we cannot ignore the fact that DON is also synthesized and released by microorganisms and algae. Thus, in ZIPGEM at EV9, for the class of  $\text{C}_n\text{H}_m\text{O}_p\text{N}_3$  and  $\text{C}_n\text{H}_m\text{O}_p\text{N}_4$ , the species with the highest relative abundance in the effluents have a higher molecular weight and a more sophisticated compound structure than in the influents (i.e.  $\text{C}_{27}\text{H}_{29}\text{N}_3\text{O}_{14}$  (618.16Da), in the effluent of cell 1 >  $\text{C}_{23}\text{H}_{23}\text{N}_3\text{O}_{12}$  (532.12Da), in the influent of cell 1;  $\text{C}_{26}\text{H}_{29}\text{N}_3\text{O}_{13}$  (590.16Da), in the effluent of cell 2 >  $\text{C}_{23}\text{H}_{23}\text{N}_3\text{O}_{12}$  (532.12Da), and in the influent of cell 2; this also applies to  $\text{C}_n\text{H}_m\text{O}_p\text{N}_4$  for cell 1 and cell 2. This can also be seen from the fact that the species with the lower molecular weight and the less sophisticated compound structure in  $\text{C}_n\text{H}_m\text{O}_p\text{N}_1$  and  $\text{C}_n\text{H}_m\text{O}_p\text{N}_2$  in the effluent of ZIPGEM were more abundant than the influents—i.e.  $\text{C}_{18}\text{H}_{17}\text{N}_1\text{O}_{10}$  (406.08Da) in the effluent of cell 1 <  $\text{C}_{18}\text{H}_{19}\text{N}_1\text{O}_{10}$  (408.09Da), in the influent of cell 1;  $\text{C}_{20}\text{H}_{22}\text{N}_2\text{O}_{10}$  (449.12Da), in the effluent of cell 1 <  $\text{C}_{21}\text{H}_{22}\text{N}_2\text{O}_{10}$  (532.12Da), and in the influent of cell 1; this applies to  $\text{C}_n\text{H}_m\text{O}_p\text{N}_4$ , and also to cell 2 for  $\text{C}_n\text{H}_m\text{O}_p\text{N}_1$  and  $\text{C}_n\text{H}_m\text{O}_p\text{N}_2$ ). Moreover, this conversion of  $\text{C}_n\text{H}_m\text{O}_p\text{N}_1$  and  $\text{C}_n\text{H}_m\text{O}_p\text{N}_2$  into  $\text{C}_n\text{H}_m\text{O}_p\text{N}_3$  and  $\text{C}_n\text{H}_m\text{O}_p\text{N}_4$  is more pronounced in the wet than in the dry season. The impact of specific seasonal effects will be discussed in Section 4.1. Fig. S4 has a comparative analysis for EV3.

At EV3 (Fig. 5), for all cells, the proportion of  $\text{C}_n\text{H}_m\text{O}_p\text{N}_1$  in the influents was higher than in the effluents, though  $\text{C}_n\text{H}_m\text{O}_p\text{N}_2$  remained essentially constant in the influents and effluents for all cells. The same applies to  $\text{C}_n\text{H}_m\text{O}_p\text{N}_3$ , whereas for  $\text{C}_n\text{H}_m\text{O}_p\text{N}_4$ , both cell 3 and cell 4 showed a higher proportion of  $\text{C}_n\text{H}_m\text{O}_p\text{N}_4$  in the effluents than in the influents, though this was not the case for cell 1 and cell 2.

At EV9 (Fig. 6), the proportion of  $\text{C}_n\text{H}_m\text{O}_p\text{N}_4$  in both the influents and effluents was much higher than in EV3. In cell 1 and cell 2, the proportion of  $\text{C}_n\text{H}_m\text{O}_p\text{N}_1$  in the influents was higher than that in the effluents, whereas in cell 3 and cell 4, the proportion of  $\text{C}_n\text{H}_m\text{O}_p\text{N}_1$  in the influents was lower than its proportion in the effluents. The same applies to  $\text{C}_n\text{H}_m\text{O}_p\text{N}_2$  and  $\text{C}_n\text{H}_m\text{O}_p\text{N}_3$ ; i.e., the proportions of  $\text{C}_n\text{H}_m\text{O}_p\text{N}_1$ ,  $\text{C}_n\text{H}_m\text{O}_p\text{N}_2$ , and  $\text{C}_n\text{H}_m\text{O}_p\text{N}_3$  in the effluents of the ZIPGEM-filled cells were all lower than that in the influents.  $\text{C}_n\text{H}_m\text{O}_p\text{N}_4$ , in contrast, showed a higher proportion in the effluents than in the influents in all the cells.

Based on the Van Krevelen diagram, the influents were associated with lignins, condensed aromatics, carbohydrates, and tannins during the dry season (EV3, Fig. S5), whereas the effluents were associated with lignins, carbohydrates, proteins, condensed aromatics, and tannins. The categories and the abundance of DON compounds in the influents, especially for lignins, in the wet season (EV9, Fig. 7) was like that in the dry season. However, the clustering of protein and carbohydrates in the effluents was denser than in the dry season.

For each cell, even though  $\text{C}_n\text{H}_m\text{O}_p\text{N}_1$  was dominant in the influent and in the effluent, the proportion of  $\text{C}_n\text{H}_m\text{O}_p\text{N}_4$  was significantly higher in the effluents than in the influents. This could be due to the intensive microbial metabolism because microorganisms do not only consume simple compounds but also produce complex compounds.

In the dry season (Fig. 5), effluents had more complex compounds ( $\text{C}_n\text{H}_m\text{O}_p\text{N}_4$ ) than that in wet season. This is consistent with the seasonal effect because in the dry season, microbial activities were less intense than in the wet season because of the limitations of energy and food, along with other environmental factors. Also, in the wet season (Fig. 7), even though lignins were one of the main components of all the effluents, simple compounds ( $\text{C}_n\text{H}_m\text{O}_p\text{N}_1$  and  $\text{C}_n\text{H}_m\text{O}_p\text{N}_2$ ) were dominant in ZIPGEM, whereas  $\text{C}_n\text{H}_m\text{O}_p\text{N}_3$  was dominant in CPS. This implies that microbial activities in aminization were more intensive in ZIPGEM than in the CPS and they can consume more DON, resulting in the sample DON compound in the effluents.

Oxygen also played an important role in understanding the filtration cell conditions that categorized the Krevelen diagrams in three zones (Bahureksa et al., 2022). These molecules with an O/C ratio  $\leq 0.3$  represented a low relative abundance of oxygen. Molecules that were  $0.3 < \text{O/C} \leq 0.6$  and  $\text{O/C} > 0.6$  indicated mid-oxygen and high-oxygen levels, respectively (Fig. 7 and Fig. S5). The target genes in this study indicated different metabolic pathways, in which denitrification and DNRA required DON produced close to anaerobic conditions (van Spanning et al., 2007).

Carrera et al. (2004) and Ling and Chen (2005) confirmed that an exponential decrease in nitrification rate was observed when the C/N ratio increased, especially when C/N was higher than 1.11 (COD/N = 3). In other words, an exponential increase in the nitrification rate was observed when the N/C ratio increased. Sun et al. (2020) also confirmed that when C/N was higher than 5, there was no AOB detectable, while the relative abundance of NOB was also low. Therefore, nitrifiers have a slow growth rate under N/C (N/C = [0.2, 0.89]), with the growth rate between this range of N/C being almost stable ( $0.4 \text{ g m}^{-2} \cdot \text{d}^{-1}$  or  $0.8 \text{ g m}^{-2} \cdot \text{d}^{-1}$ ) (Carrera et al., 2004; Ling and Chen, 2005). However, when the N/C is higher than 1, the growth rate of nitrifiers can exponentially increase as N/C increases. Even so, such an exponential increase does not mean nitrifiers are comparable to denitrifiers. For example, Sun et al. (2020) demonstrated that the relative abundance is 10.5% for NOB and 0.03% for AOB, even when C/N = 0.

Bi et al. (2015) demonstrated that when N/C is lower than 0.3, the denitrification rate is stable for denitrifiers, which can remove 70% of TN. When N/C is higher than 0.3 but lower than 0.6, as N/C increases,



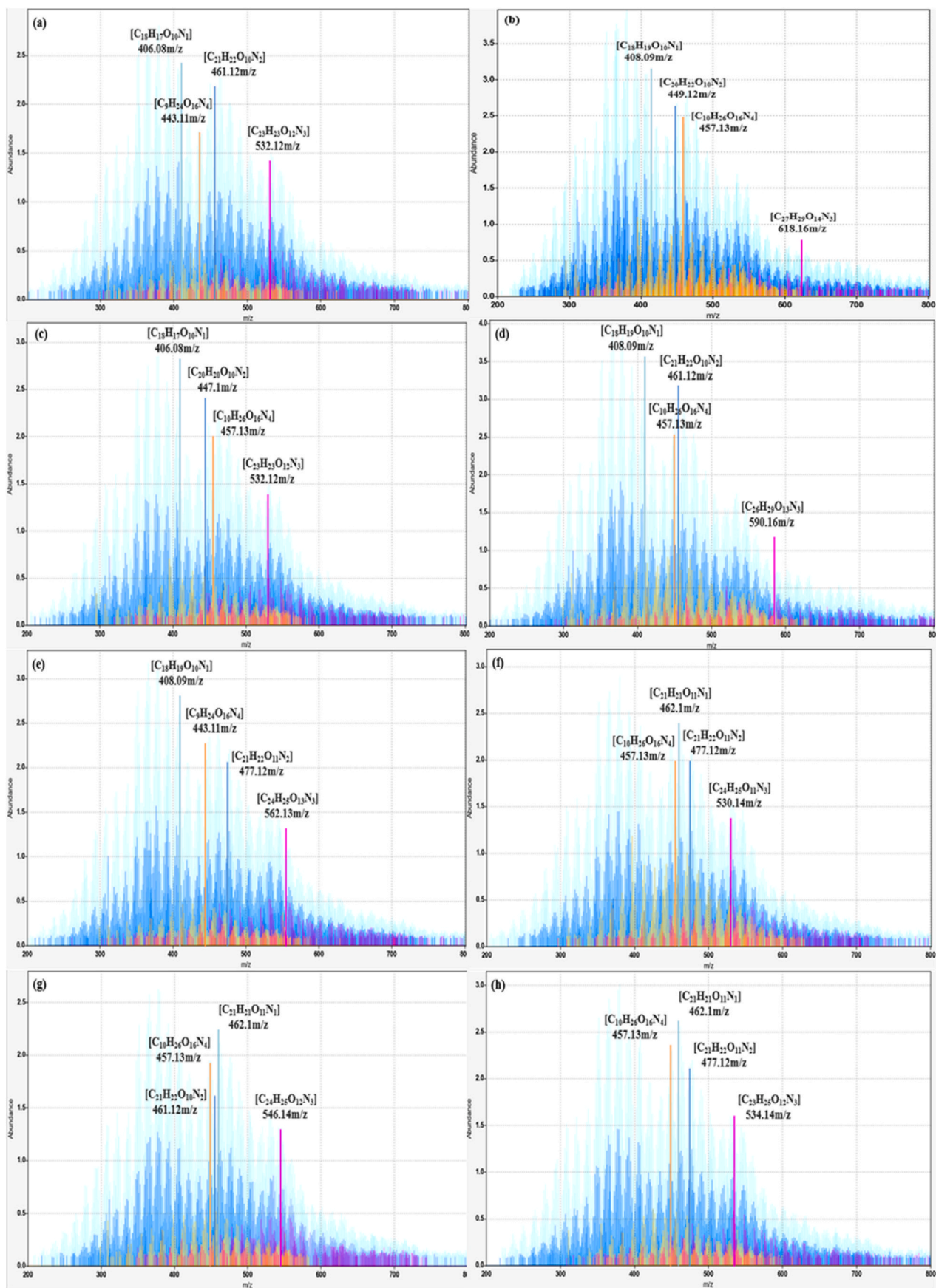


Fig. 4. 21 T (-) ESI FT-ICR MS analysis of DON in the influents and effluents at EV9: (a) influent of cell 1; (b) effluent of cell 1; (c) influent of cell 2; (d) effluent of cell 2; (e) influent of cell 3; (f) effluent of cell 3; (g) influent of cell 4; and (h) effluent of cell 4.

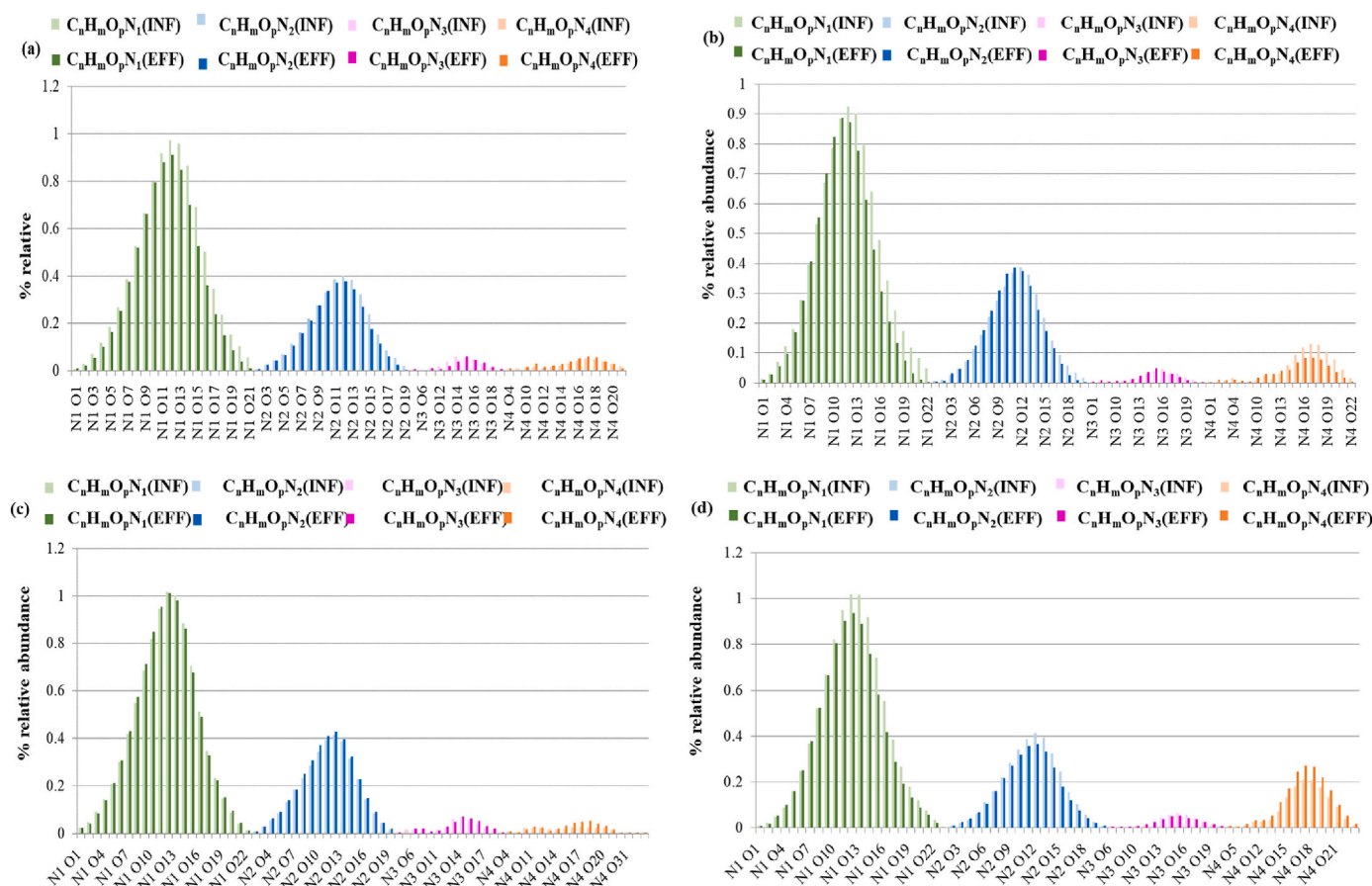


Fig. 5. Relative abundance of classes of influent vs. effluent for ZIPGEM and CPS during event 3 including (a) ZIPGEM in cell 1; (b) ZIPGEM in cell 2; (c) CPS in cell 3; and (d) CPS in cell 4.

the denitrification rate increases while achieving the maximum at N/C = 0.6, which can remove nearly 95% of TN. When N/C is higher than 0.6, as this ratio increases, the denitrification rate decreases but still can remove 40% of TN. The above finding is also consistent with Mohan et al. (2016), in which an N/C ratio of 0.67 was optimal for the denitrification of high-strength nitrate wastewater.

For Anammox, Bi et al. (2015) also found that when N/C is lower than 0.25, the growth rate of Anammox is minimal. When the ratio is between 0.25 and 0.67, the growth rate of Anammox also increases as the ratio increases; however, when the ratio is higher than 0.67, as the ratio increases, the growth rate of Anammox decreases. S. Liu et al., (2021) demonstrated that as the ratio of N/C (between 0.08 and 0.5) increases, the rate of DNRA decreases. Yoon et al. (2015) confirmed that from an N/C ratio of 0.13–0.22, the rate of DNRA decreases as the ratio increases. Also, when N/C is higher than 0.33, the growth of DNRA is minimal. Therefore, the lower the N/C is, the higher the growth rate of DNRA is given sufficient ammonium (S. Xu et al., 2020). This finding is also consistent with H. Liu et al., (2021) and He et al. (2022), in which there is a significant positive relationship between the growth rate of Comammox and the ratio of N/C. Ye et al. (2024) also confirmed that with the ratio of N/C between 0.066 and 0.2, the growth rate of Comammox increases, more rapidly than nitrification.

Fig. 8 and Fig. S6 plot the Van Krevelen diagrams of H/C against the N/C ratio at EV9 and EV3, respectively. The diagram was edited based on the experimental data of this study: ① with N/C between 0 and 0.08, the order of growth rate was nirS > Anammox > Comammox; ② with N/C between 0.08 and 0.15, the order of the growth rate was DNRA > nirS > Comammox > Anammox; ③ with N/C between 0.15 and 0.2, the order of the growth rate was nirS > DNRA > Comammox > Anammox; ④ with N/C between 0.2 and 0.3, the order of the growth rate was nirS

> DNRA > Anammox > NOB > AOB; ⑤ with N/C between 0.3 and 0.67, the order of growth rate was nirS > Anammox > NOB > AOB; ⑥ with N/C between 0.67 and 1, the order of growth rate was nirS > Anammox > NOB > AOB; and ⑦ with N/C between higher than 1, the order of growth rate was NOB > AOB > nirS > Anammox.

#### 4.4. Biodegradability of DON

According to Fig. S7, BDON's percentage was approximately 42% of DON in the influents during the dry season (EV3) and 45% of DON in the influents during the wet season (EV9), affirming an increase in BDON's share in the wet phase owing to heightened DO and nutrient contributions. Yet, during the dry season, the percentage of BDON in cells 1 and 2, namely those filled with ZIPGEM, fell from 42% in the influents to 30% in the effluents, whereas in the wet season, it fell from 45% in the influents to 5–10% in the effluents. In the case of cells 3 and 4, specifically those filled with CPS, BDON was eliminated in a mere 1–5% during the dry season, whereas BDON's percentage in the effluents stayed close to 20% in the wet season, a figure just about 25% less than that in the influents.

#### 4.5. Population dynamics of microbial species

An assessment of the population density for microbial ecology, responsible for the nitrogen cycle, was conducted using qPCR for ZIPGEM and CPS during EV3 (dry season) and EV9 (wet season). The key participants, categorized by population densities, included AOB, NOB, nirS, Anammox, DNRA (nrfA), Comammox, and IRB. Upon analyzing the population densities of the mentioned bacteria, the sequence was nirS (10 million copies/g dry mass) > nrfA (million copies/g dry mass) > IRB

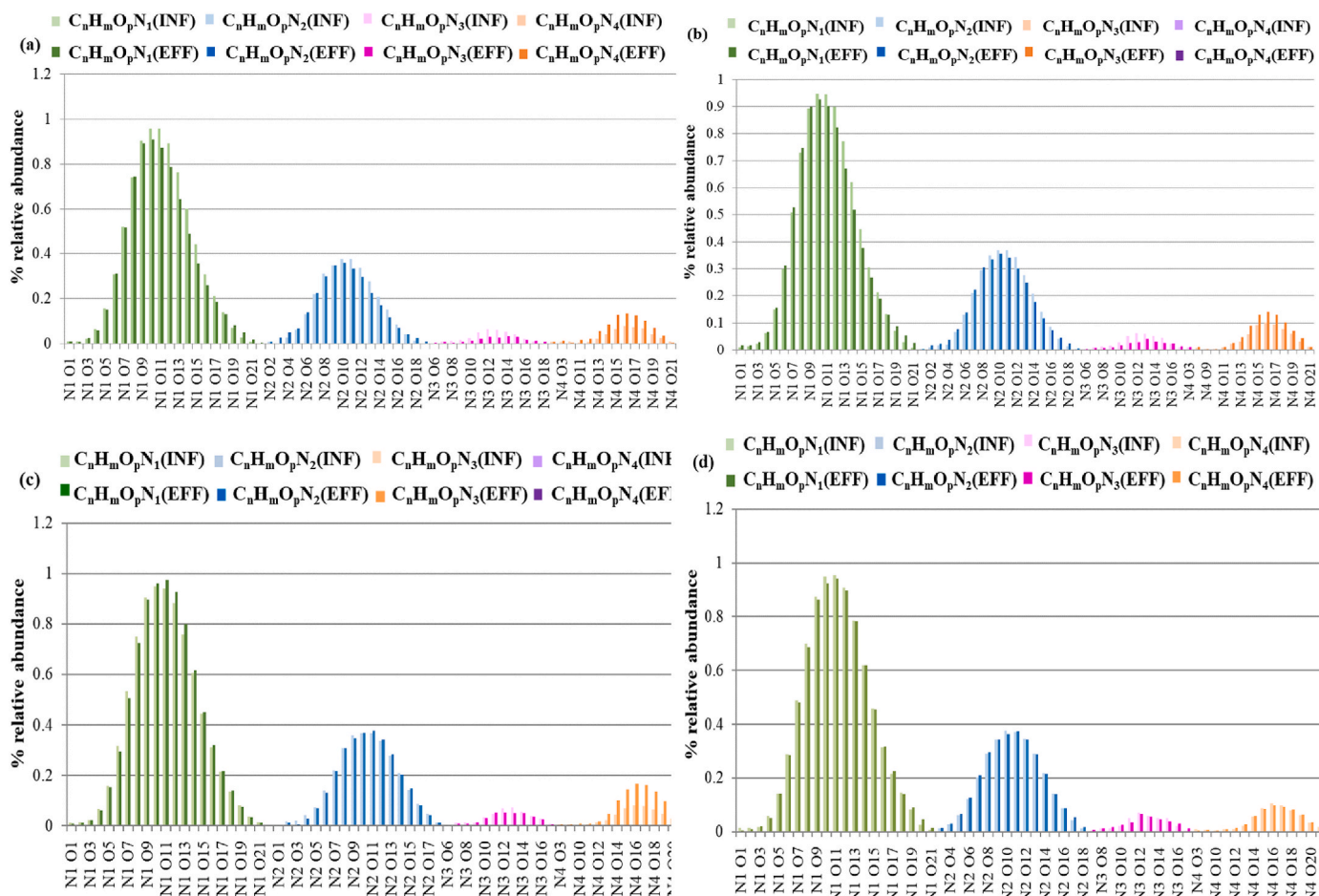


Fig. 6. Relative abundance of classes for influent vs. effluent for ZIPGEM and CPS during event 9 including (a) ZIPGEM in cell 1; (b) ZIPGEM in cell 2; (c) CPS in cell 3; and (d) CPS in cell 4.

(above 10 thousand copes/g dry mass) > Comammox (below 10 thousand copies/g dry mass) > Anammox (thousand copies/g dry mass) > AOB or NOB (hundred copies/g dry mass; Fig. S8). Consequently, the primary nitrogen (N) cycling mechanisms in the filtration system were denitrification and the conversion of dissimilatory nitrate to ammonium, proving the robustness of  $\text{NO}_3^-$  respiration (where  $\text{NO}_3^-$  is converted to  $\text{NO}_2^-$ ).

Denitrification denotes the biochemical transformation in which nitrogen in nitrate ( $\text{NO}_3^-$ ) is converted into nitrogen gas by microbes via a sequence of intermediary products, namely nitrite ( $\text{NO}_2^-$ ), nitric oxide (NO), and nitrogen oxide ( $\text{N}_2\text{O}$ ). Consequently, the denitrification procedure is composed of four distinct modular phases, each facilitated by nitrate reductase, nitrite reductase, nitric oxide reductase, and nitrous oxide reductase, in that order, with the respective coding genes nar (eq. (4)), nir (eq. (5)), nor (eq. (6)), and nos (eq. (7); Fig. 9) (Sun and Jiang, 2022):



The second step in the denitrification process is the reduction of  $\text{NO}_2^-$  to NO, which distinguishes denitrification from other nitrate metabolisms and is an essential rate-limiting step of denitrification (Jiang et al.,

2017; Maria et al., 2020). Here, the population of nirS was exceptionally high (more than 10 million copies), proving the denitrification rate was very high. DNRA consists of two steps ( $\text{NO}_3^- \rightarrow \text{NO}_2^- \rightarrow \text{NH}_4^+$ ), even though it shares the same first step with denitrification; however, under anaerobic conditions, in the absence of  $\text{O}_2$ , DNRA has an advantage over denitrification because it transfers eight electrons compared to only five during denitrification (eq. (8) and eq. (9)) (Pandey et al., 2020). At lower C/N ratios (the proportion of C atoms in the electron donor to N atoms in the electron acceptor), denitrification was the primary process (i.e., electron donor-limiting growth conditions), in contrast to DNRA, which was the main outcome at higher C/N ratios (i.e., electron acceptor-limiting growth conditions) (Yoon et al., 2015; S. Xu et al., 2020; Pandey et al., 2020). This may explain why nrfA was the second largest group in the filtration system. This could also partly explain why the removal percentage of ammonia nitrogen was negative in the wet season. After comparing nirS and nrfA, it seems nrfA prefers CPS, and nirS prefers ZIPGEM; this can be explained by adding ZVI in the ZIPGEM cells. Ma et al. (2021) demonstrated that  $\text{Fe}^{2+}$  could stimulate denitrifier metabolism and growth, elevate denitrifying gene abundance, and increase denitrifying enzymes. However, for CPS, even though the population density of nirS was still higher than that of nrfA, the population of nrfA in CPS was higher than that in ZIPGEM cells. This is consistent with algal growth and the ratio of C/N. Drift algae's emission and breakdown serve as sources of organic carbon (C) for processes like denitrification and DNRA. Furthermore, the buildup of decomposing substances may prevent oxygen from entering the filtration system, thus fostering an environment conducive to the reduction of heterotrophic nitrate. It is well known that the high ratio of organic carbon to nitrate usually favors



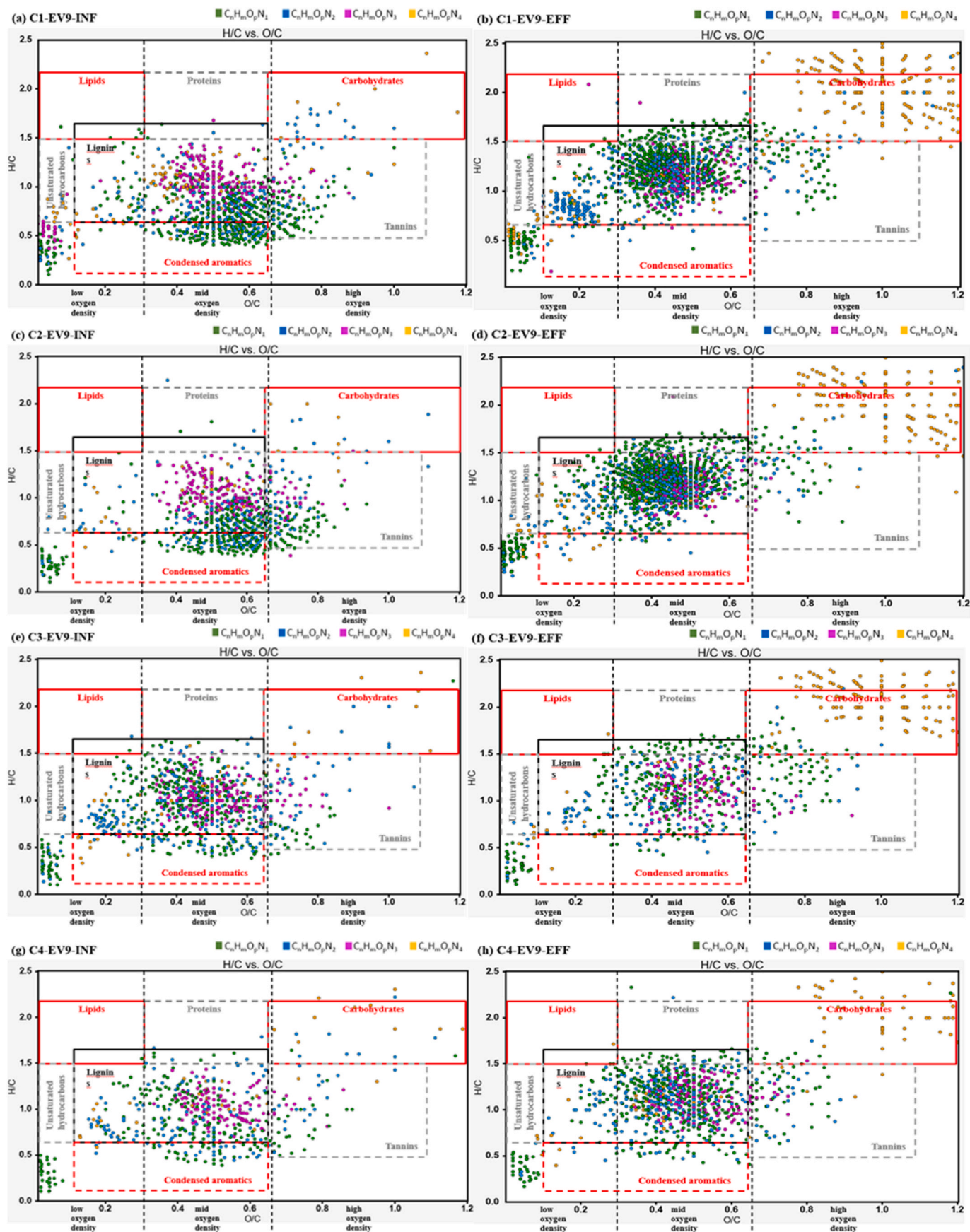


Fig. 7. Van Krevelen diagrams for ZIPGEM and CPS during event 9 (EV9) including (a) influent of ZIPGEM in cell 1; (b) effluent of ZIPGEM in cell 1; (c) influent of ZIPGEM in cell 2; (d) effluent of ZIPGEM in cell 2; (e) influent of CPS in cell 3; (f) effluent of CPS in cell 3; (g) influent of CPS in cell 4; and (h) effluent of CPS in cell 4.

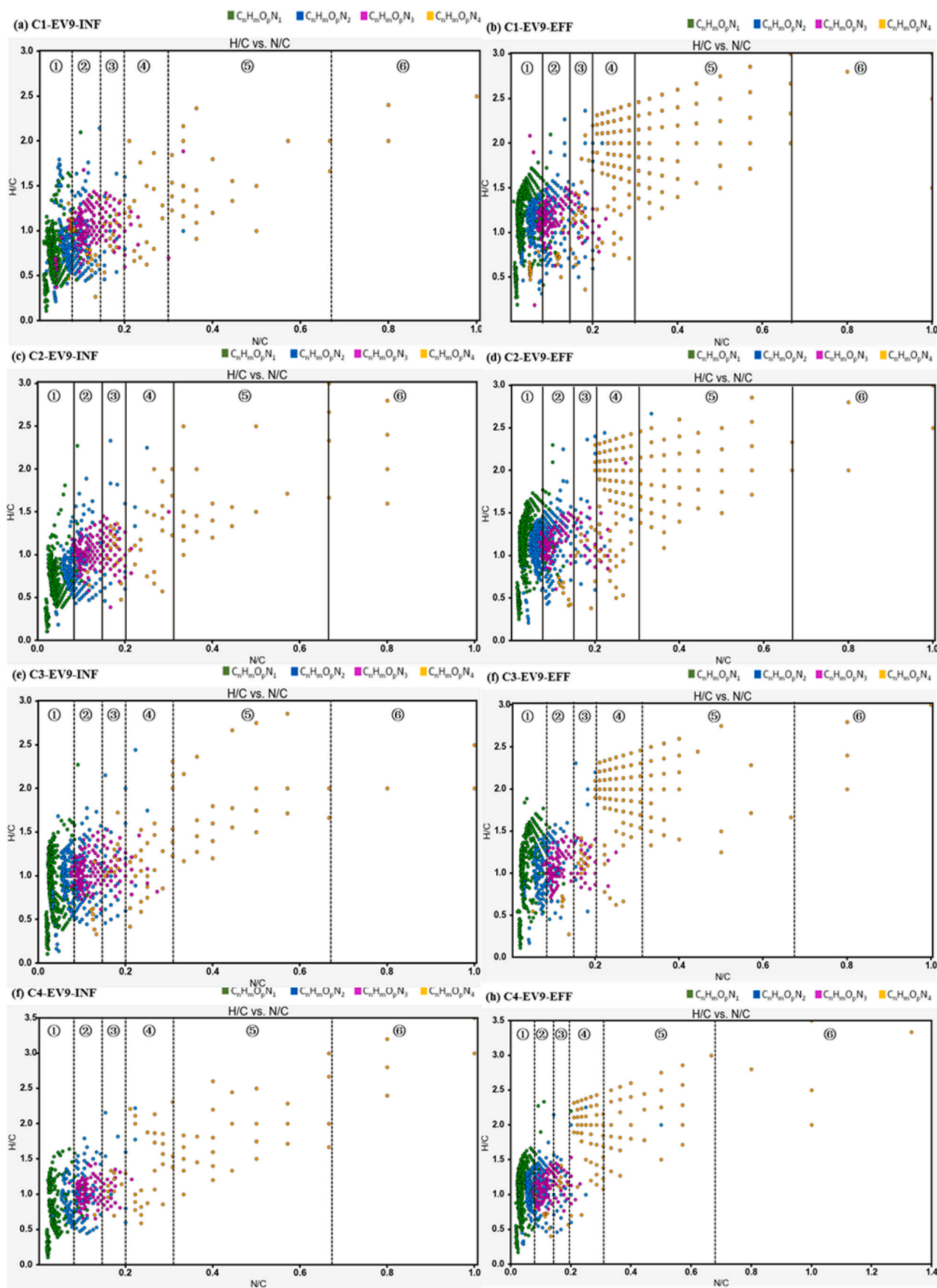


Fig. 8. Relation between N/C ratio diagrams with microbial metabolic pathways at event 9: (a) influent of cell 1; (b) effluent of cell 1; (c) influent of cell 2; (d) effluent of cell 2; (e) influent of cell 3; (f) effluent of cell 3; (g) influent of cell 4; and (h) effluent of cell 4.

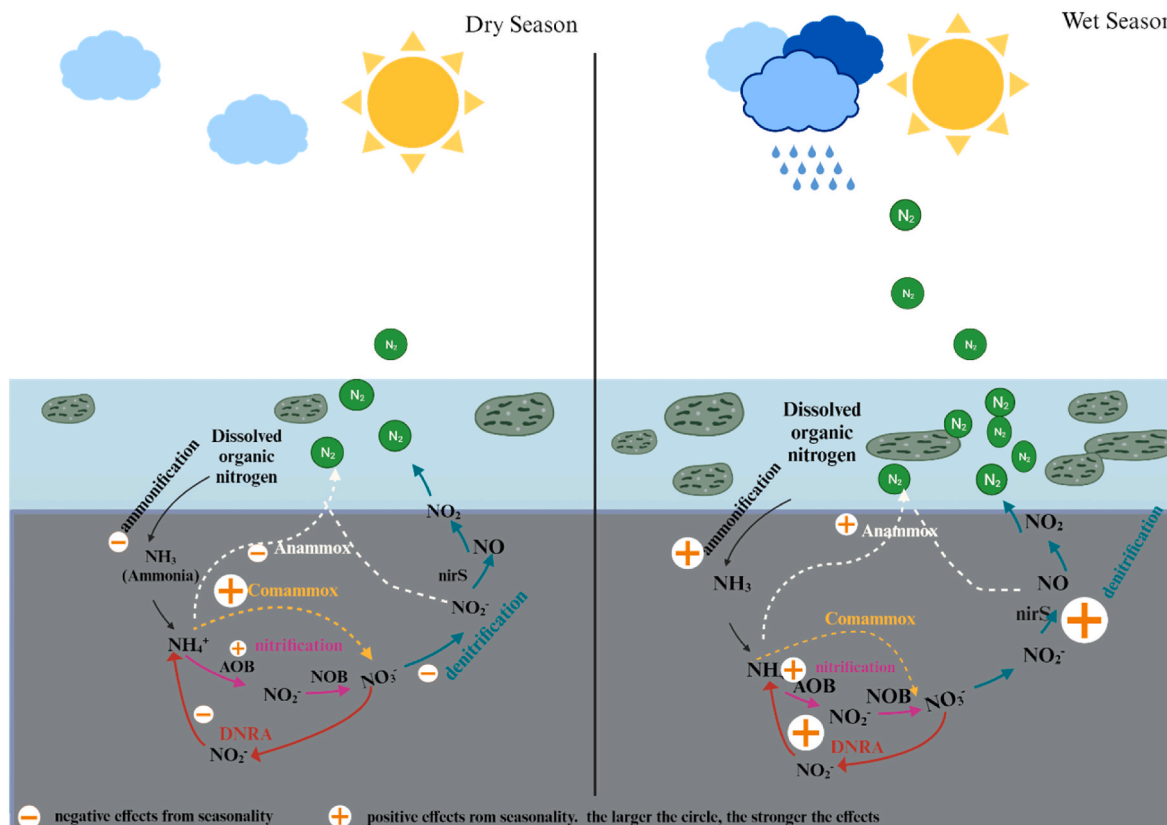
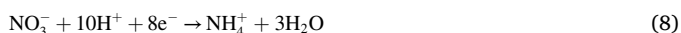


Fig. 9. The nitrogen cycle in the media bed affected by the seasonality effect.

DNRA over denitrification (Jiang et al., 2023). Compared to CPS, ZIPEM was better at removing nutrients. Therefore, more organic carbon is kept in CPS; therefore, higher C/N favors DNRA. In a word, this highly organic and eutrophic canal water system favors DNRA.

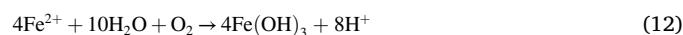


Almost every type of bacteria increases significantly in the wet season; however, Comammox is the only one that gains a better population density in the dry season, especially in nitrifiers. Therefore, Comammox bacteria were the main driver of nitrification in the filtration system. This can be explained by the fact that common bacteria have a wider ecological niche than other nitrifiers (AOA, AOB, and NOB) (Ye et al., 2024), enabling them to survive in environments with limited nutrient conditions. This may explain why Comammox was dominant in the nitrifiers.

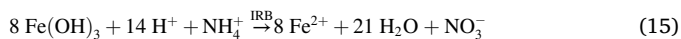
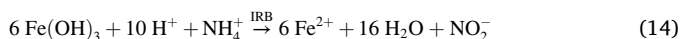
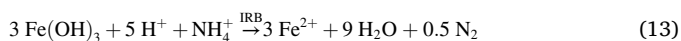
Anammox mostly thrived in the 1-foot medium. Amazingly, the Anammox population increased even at the top of the cells from the dry season to the wet season, proving that oxygen was limited at the top of the layer. This is why the biofilm has more intensive growth in the wet season and consumes nitrogen and depletes oxygen at the top. The population quantity of AOB was significantly lower in EV3 (dry season) and higher in EV9 (wet season). This phenomenon was discovered and quantified by qPCR at the top of all the cells. The population of NOB in ZIPGEM increased more significantly than CPS from EV3 to EV9, with the highest quantities at the top.

Fe, crucial for microorganisms, has the potential to enhance the activity of microbial metabolic enzymes; promote stimulate intracellular, extracellular, and interspecies electron transfers; and boost the production of extracellular polymeric substances in bacteria (Y. Liu et al., 2023). The exogenous Fe in the filtration system needed to drive the Fe-N cycle may facilitate an efficient strategy to improve biological N

removal efficiency. In fact, a variety of biological nitrogen removal methods for wastewater, including Anammox, nitrification, and denitrification, are known to utilize Fe (Chen et al., 2021; Hu et al., 2022; Li et al., 2023). ZVI can act as an electron donor; pollutants act as electron acceptors; and a redox reaction occurs. Placing ZVI in the ZIPGEM cells can reduce the redox potential of the filtration system and spur the growth of anaerobic microorganisms because ZVI can slowly release  $\text{Fe}^{2+}$  into the water, consume dissolved oxygen, and promote the metabolic growth of Anammox and denitrifiers. In detail, for Anammox, ZVI can rapidly oxidize to the advantageous ions of  $\text{Fe}^{2+}$  (eq. (10) or eq. (11)), which will be further oxidized into  $\text{Fe}(\text{OH})_3$  (eq. (12)) (Wang et al., 2021). The  $\text{Fe}^{2+}$  and  $\text{Fe}^{3+}$  will not only aggregate Anammox but also increase N removal and create the optimal redox potential environment for Anammox growth (Gao et al., 2014). For nitrification and denitrification, Fe can be used as the active center of functional enzymes in the nitrification (enzymes include ammonia monooxygenase [AMO] and nitrite oxidoreductase) and denitrification (periplasmic nitrate reductase and nitrite reductase) processes, and as an electron acceptor for electron transport chains and auxiliary groups related to cellular metabolism to improve bacterial metabolic activity and thus N conversion efficiency by nitrifiers and denitrifiers (Chen et al., 2018). In addition, IRB such as *Geobacter* can engage in the Feammox process, in which  $\text{NH}_4^+$  is oxidized to  $\text{N}_2$ ,  $\text{NO}_2^-$ , or  $\text{NO}_3^-$ , and  $\text{Fe}^{3+}$  is reduced to  $\text{Fe}^{2+}$  as shown in eqs. (13)–(15). During this process, IRB can be capable of utilizing various electron donors to reduce  $\text{Fe}^{3+}$  (hydro)oxides extracellularly.







## 5. Discussion

### 5.1. Seasonal effect on microbial community

Nitrogen cycling in aquatic systems is not only affected by changes in climatic conditions but also by the impression of human activities. For example, changes in climatic conditions not only affect the length and intensity of the dry and wet seasons (Fill et al., 2019), but human activities, especially agricultural production activities, affect the nitrogen content of the water body and the content of organic matter (Xenopoulos et al., 2021) as well as habitat factors such as the oxygen and pH changes with the alternation of the wet and dry seasons (Y. Chen et al., 2022). Our project is in the South Florida region, where the nitrogen cycle in surface waters is closely linked to climate, hydrology, and human activities. For example, in the St. Lucie Estuary, in addition to discharges from Lake Okeechobee (south Florida), the N and P enrichment emanating from septic systems through shallow groundwaters also contribute to nutrient pollution and harmful algal blooms (Lapointe et al., 2017).

Warmer water and nutrient-rich runoff in the wet season can lead to algal blooms. Algal blooms can deplete DO levels, which can favor denitrification, DNRA, and Anammox. In the dry season, cooler temperatures can result in higher DO concentrations, favoring nitrification and Comammox, because temperatures are slightly lower than in the wet season. However, in the dry season, the amount of ammonia is limited. This corroborates the finding that ZIPGEM and CPS in the first four sampling events showed positive ammonia removal percentages. As a result, the increase in the population of AOB bacteria was not significant, and because NOB is highly dependent on the product of AOB, i.e., nitrite, the population of NOB was even less significant than that of AOB. Comammox is favored among nitrifiers in the dry season, which is consistent with Zheng et al. (2022) Comammox possesses a unique cytochrome bd-like terminal oxidase, potentially allowing greater oxygen attraction compared to AOB (Costa et al., 2006). Consequently, the plentiful presence of Comammox bacteria might mitigate the negative impact of insufficient dissolved oxygen on the total nitrification efficiency (Liu and Wang, 2013; Roots et al., 2019). Conversely, because of the arrival of wet season, the decrease in DO and the accumulation of more nitrate realized a significant increase in the populations of nirS, DNRA, and Anammox in the wet season.

In summary, seasonal effects were evident in the media of ZIPGEM and CPS, mainly through the inhibition of denitrification, DNRA, and Anammox in the dry season because these three processes required an anaerobic environment. In the dry season, the dissolved oxygen content in the water was higher because there were fewer aquatic algae. In contrast, the exuberant aquatic algae and higher organic matter content in the wet season depleted the dissolved oxygen in the water, which further created an anaerobic environment at the top and inside the media (ZIPGEM and CPS), thus stimulating the growth of nirS, nrfA, and Anammox. The nitrification process requires oxygen, so in the dry season, fewer nutrient inputs resulted in higher levels of dissolved oxygen in the water, which led to a certain intensity of nitrification reactions in both ZIPGEM and CPS, especially of Comammox. However, in the wet season, although rainfall increased in frequency compared to the dry season, thus boosting the oxygen concentration in the water, the exuberant algal species consumed most of the oxygen, which led to an insignificant increase in the intensity of nitrification reactions, as is directly manifested by the fact that AOB and NOB also did not increase significantly in the wet season. Tables S10 and S11 list dissolved oxygen

(mg/L) and pH in the influents and effluents between event 2 and event 9, confirming that the concentration of dissolved oxygen in the effluents in the dry season is higher than in the wet season.

### 5.2. Seasonal effect on DON concentration and composition and on BDON

Dissolved organic nitrogen contained in the inlet stream in the dry season was lower than that in the inlet stream in the wet season, at 1.748 mg L<sup>-1</sup> and 2.444 mg L<sup>-1</sup>, respectively. This proves that nutrient inputs in the wet season were greater than in the dry season (Table S12). Comparing the whole spectrum, we find that, in the influents and effluents, the number of oxygen atoms, carbon atoms, and carbon atoms in four classes of DON (i.e. C<sub>n</sub>H<sub>m</sub>O<sub>p</sub>N<sub>1</sub>, C<sub>n</sub>H<sub>m</sub>O<sub>p</sub>N<sub>2</sub>, C<sub>n</sub>H<sub>m</sub>O<sub>p</sub>N<sub>3</sub>, and C<sub>n</sub>H<sub>m</sub>O<sub>p</sub>N<sub>4</sub>) substances show a decreasing trend from the dry season (EV3) to the wet season (EV9), which indicates a decrease in the structural complexity of DON from the dry to the wet season, indirectly corroborating the common assumption that the metabolism of microorganisms is vigorous in the wet season (EV9). Similarly, the molecules with the highest proportion of DONs in each class of DONs also showed a decreasing trend; for example, the molecular weight of C<sub>n</sub>H<sub>m</sub>O<sub>p</sub>N<sub>1</sub> decreased from [476.12Da, 542.13Da] in the dry season (EV3) to [406.08Da, 462.1Da] in the wet season (EV9). The molecular weight of C<sub>n</sub>H<sub>m</sub>O<sub>p</sub>N<sub>4</sub> decreased from [469.09 Da, 571.2 Da] in the dry season (EV3) to [443.11 Da, 457.13 Da] in the wet season (EV9). Moreover, in the wet season, all the effluents of ZIPGEM showed lower molecular weights and less structural complexity than the effluents of CPS, proving that the bacterial metabolic activities were more intensive in the medium of ZIPGEM in the wet season. In the dry season, DON's molecular weight and structural complexity in the effluents of CPS were much higher than those of ZIPGEM and higher than those of CPS in the wet season.

During the dry season, proteins and carbohydrates increased in the effluents, whereas condensed aromatics decreased in the influents in which the proteins is aliphatic and typically represents the bulk of the labile DON pool. In contrast to the proteins, the lignins, among the major components of the semi-labile and refractory DON pools, presumably have an aromatic nature that limits their degradability. However, anaerobic heterotrophs can utilize aromatic compounds in the absence of oxygen as carbon or energy sources for microbes (Gibson and Harwood, 2002). This finding is consistent with our qPCR results because there was limited oxygen, when many anaerobic microbes were cultivated including nirS, nrfA, and Anammox.

During the wet season, the clustering of protein and carbohydrates in the effluents is denser than that in the dry season. This can be attributed to photosynthetic microorganisms, which can fix carbon dioxide through photosynthesis to produce various organic biomolecules including carbohydrates and proteins (Xu et al., 2008). This finding is consistent with our observation in the wet season, when dense biofilm growth is robust because microorganisms metabolize carbohydrates and produce proteins inside the media, as opposed to the dry season when biofilms are still in the stage of formation.

### 5.3. Linking DON decomposition with microbial population dynamics

In the bioactive filtration system (Law et al., 2012), the organic components of dissolved organic nitrogen, including proteins, amino acids, and amino sugars, undergo immediate degradation into ammonium (NH<sub>4</sub><sup>+</sup>). The decomposition process for proteins entails the hydrolysis of peptide bonds, leading to the release of amino acids. Subsequently, amino acids undergo deamination into ammonium, facilitated by various enzymes known as deaminases. Various amino acids engage distinct deaminases, such as glutamate dehydrogenase (Xian et al., 2020; Z. Chen et al., 2022), serine dehydratase (Kuroda et al., 2021), threonine dehydratase (Choi, 2021), and alanine deaminase (Bei et al., 2023).

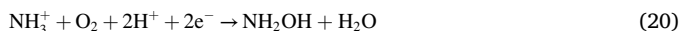
Additionally, the synthesis of urea ( $\text{CH}_4\text{N}_2\text{O}$ ) and cyanate ( $\text{CNO}^-$ ) occurs through the oxidation of amino acids and ammonia, serving as substitute electron donors for AOB and NOB in scenarios where free ammonia is scarce. (Spang et al., 2012; Sonthiphand and Neufeld, 2014; Mundinger et al., 2019). Besides nitrification, Anammox can break down cyanate and urea (eq. (16) and eq. (17)) (Palatinszky et al., 2015; Ganesh et al., 2018), utilizing these substances as an energy source for metabolic activity. Recent studies have shown urea to be the predominant LDON (labile-dissolved organic nitrogen) utilized by AOB, NOB, and Comammox (Q. Liu et al., 2023), which are characterized by their distinct urea transporter genes (AOB: utp; NOB and Comammox: urtABCDE and utp) along with the urease genes ureABC. Phytoplankton (Zumft, 1997; Bradley et al., 2010; Highton et al., 2020) is also capable of bio-assimilating low molecular weight DON substances such as urea and amino acids.



Nitrification involves a two-step process of aerobic biological oxidation. The initial step in the velocity-limiting process involves ammonia transforming into nitrite, a process executed by AOB (eq. (18)). The swift second phase involves transforming nitrite into nitrate, a process executed by NOB (eq. (19)).



AOB bacteria initiate the nitrification process, also known as nitrification, involving a two-stage process with hydroxylamine ( $\text{NH}_2\text{OH}$ ) as the intermediary. Nitrification begins with the conversion of ammonia into hydroxylamine, a process facilitated by the membrane anchored enzyme ammonia monooxygenase that catalyzes the oxidation of  $\text{NH}_4^+$  to  $\text{NH}_2\text{OH}$  (eq. (20)). During the subsequent step, hydroxylamine undergoes additional oxidation into nitrite, facilitated by hydroxylamine oxidoreductase, utilizing water oxygen and extra molecular oxygen as the final electron acceptor (eq. (21)). In this step, two electron pairs are produced, with one pair being offset to facilitate the initial step of ammonia oxidation. Conversely, the alternate pair is transferred to the terminal oxidase through an electron transport chain, creating a proton motive force (eq. (16)) (Sinha and Annachhatre, 2007).



## 6. Conclusion

DON plays an important role in surface water eutrophication. Because microorganisms are intimately associated with DON transformation, bioactivated green sorption media in this study were explored at the field scale to remove DON and other nitrogen species. This novel field-scale study proves the technical feasibility of large-scale best management practices (BMPs), especially in the environment of South Florida, where the Everglades—the largest subtropical wilderness in the United States—is very sensitive to human activities and climate change. Even though DON's conversion and biodegradability are affected by environmental factors and molecular weight size, hydrophilicity and hydrophobicity, and the charge characteristics of DON, this water filtration system provides a friendly substrate (hot pot) for microbial growth. Therefore, given the complexity of DON, the green sorption media (ZIPGEM) may become one of the BMPs to remove DON in the future. Through this five-month field study of the application of a

sustainable technology, ZIPGEM demonstrated better nitrogen removal than CPS. It is indicative that the material sustainability of the two filtration media is highly related to their design matrixes, as confirmed by their material characterizations, and both green sorption media could be used as soil amendments to increase soil fertility and enhance the diversity of the microbial ecology in different soils.

## CRedit authorship contribution statement

**Jinxiang Cheng:** Writing – original draft, Validation, Investigation, Formal analysis, Data curation. **Alejandra Robles-Lecompte:** Formal analysis, Data curation. **Amy M. McKenna:** Writing – review & editing, Validation, Data curation, Conceptualization. **Ni-Bin Chang:** Writing – review & editing, Validation, Supervision, Resources, Project administration, Methodology, Conceptualization.

## Declaration of competing interest

The authors declare that they have no known competing financial interests or personal relationships that could have appeared to influence the work reported in this paper.

## Data availability

Data will be made available on request.

## Acknowledgements

The authors acknowledge the financial support from the Shared Research Facilities fund at the University of Central Florida (16200710) and the Florida Department of Environmental Protection (Award ID: INV 008). A portion of this work was performed at the National High Magnetic Field Laboratory ICR User Facility, which is supported by the National Science Foundation Division of Chemistry and Division of Materials Research through DMR-2128556, (previous grant number DMR-1644779) and the State of Florida. The authors appreciate the support for field data collection from Mohamad Odeh, Diana Valencia, Diana Ordenez, and Md Touhidul Islam.

## Appendix A. Supplementary data

Supplementary data to this article can be found online at <https://doi.org/10.1016/j.chemosphere.2024.142042>.

## References

- Akkanen, J., Kukkonen, J.V., 2003. Measuring the bioavailability of two hydrophobic organic compounds in the presence of dissolved organic matter. *Environ. Toxicol. Chem.* 22, 518–524.
- Alimoradi, S., Stohr, H., Stagg-Williams, S., Sturm, B., 2020. Effect of temperature on toxicity and biodegradability of dissolved organic nitrogen formed during hydrothermal liquefaction of biomass. *Chemosphere* 238, 124573.
- Antia, N.J., Harrison, P.J., Oliveira, L., 1991. The role of dissolved organic nitrogen in phytoplankton nutrition, cell biology and ecology. *Phycologia* 30, 1–89.
- Antony, R., Grannas, A.M., Willoughby, A.S., Sleighter, R.L., Thamban, M., Hatcher, P.G., 2014. Origin and sources of dissolved organic matter in snow on the East Antarctic ice sheet. *Environ. Sci. Technol.* 48, 6151–6159.
- Azziz, G., Monza, J., Etchebehere, C., Irisarri, P., 2017. nirS-and nirK-type denitrifier communities are differentially affected by soil type, rice cultivar and water management. *Eur. J. Soil Biol.* 78, 20–28.
- Bahureksa, W., Borch, T., Young, R.B., Weisbrod, C.R., Blakney, G.T., McKenna, A.M., 2022. Improved dynamic range, resolving power, and sensitivity achievable with FT-ICR mass spectrometry at 21 T reveals the hidden complexity of natural organic matter. *Anal. Chem.* 94, 11382–11389.
- Bei, E., Ye, Z., Chen, X., Li, X., Wang, J., Qiu, Y., et al., 2023. Study on characteristic and mechanism involved in the formation of N-nitrosodimethylamine precursors during microbial metabolism of amino acids. *Sci. Total Environ.* 874, 162469.
- Berman, T., Bronk, D.A., 2003. Dissolved organic nitrogen: a dynamic participant in aquatic ecosystems. *Aquat. Microb. Ecol.* 31, 279–305.
- Bi, Z., Takekawa, M., Park, G., Soda, S., Zhou, J., Qiao, S., Ike, M., 2015. Effects of the C/N ratio and bacterial populations on nitrogen removal in the simultaneous anammox

- and heterotrophic denitrification process: mathematic modeling and batch experiments. *Chem. Eng. J.* 280, 606–613.
- Bradley, P.B., Sanderson, M.P., Frischer, M.E., Brofft, J., Booth, M.G., Kerkhof, L.J., Bronk, D.A., 2010. Inorganic and organic nitrogen uptake by phytoplankton and heterotrophic bacteria in the stratified Mid-Atlantic Bight. *Estuar. Coast Shelf Sci.* 88, 429–441.
- Bronk, D.A., See, J.H., Bradley, P., Killberg, L., 2007. DON as a source of bioavailable nitrogen for phytoplankton. *Biogeosciences* 4, 283–296.
- Carrera, J., Vicent, T., Lafuente, J., 2004. Effect of influent COD/N ratio on biological nitrogen removal (BNR) from high-strength ammonium industrial wastewater. *Process Biochem.* 39, 2035–2041.
- Chen, H., Zhao, X., Cheng, Y., Jiang, M., Li, X., Xue, G., 2018. Iron robustly stimulates simultaneous nitrification and denitrification under aerobic conditions. *Environ. Sci. Technol.* 52, 1404–1412.
- Chen, Y., Chen, R., Liu, Z., Ren, B., Wu, Q., Zhang, J., et al., 2022a. Bioretention system mediated by different dry-wet alterations on nitrogen removal: performance, fate, and microbial community. *Sci. Total Environ.* 827, 154295.
- Chen, Y., Jia, F., Liu, Y., Yu, W., Cai, W., Zhang, X., et al., 2021. The effects of Fe (III) and Fe (II) on anammox process and the Fe–N metabolism. *Chemosphere* 285, 131322.
- Chen, Z., Qiu, S., Li, M., Zhou, D., Ge, S., 2022b. Instant inhibition and subsequent self-adaptation of *Chlorella* sp. toward free ammonia shock in wastewater: physiological and genetic responses. *Environ. Sci. Technol.* 56, 9641–9650.
- Choi, K.Y., 2021. Nitrogen-neutral amino acids refinery: deamination of amino acids for bio-alcohol and ammonia production. *ChemBioEng Rev.* 8, 213–226.
- Costa, E., Pérez, J., Kreft, J.U., 2006. Why is metabolic labour divided in nitrification? *Trends Microbiol.* 14, 213–219.
- Davis, A.P., Shokouhian, M., Sharma, H., Minami, C., 2006. Water quality improvement through bioretention media: nitrogen and phosphorus removal. *Water Environ. Res.* 78, 284–293.
- Dionisi, H.M., Layton, A.C., Harms, G., Gregory, I.R., Robinson, K.G., Saylor, G.S., 2002. Quantification of Nitrosomonas oligotropha-like ammonia-oxidizing bacteria and Nitrospira spp. from full-scale wastewater treatment plants by competitive PCR. *Appl. Environ. Microbiol.* 68, 245–253.
- Dittmar, T., Stubbins, A., 2014. 12.6-Dissolved organic matter in aquatic systems. *Treatise on geochemistry* 2, 125–156.
- Dong, W., Li, W., Tao, Z., 2021. A comprehensive review on performance of cementitious and geopolymeric concretes with recycled waste glass as powder, sand or cullet. *Resour. Conserv. Recycl.* 172, 105664.
- Douterelo, I., Boxall, J.B., Deines, P., Sekar, R., Fish, K.E., Biggs, C.A., 2014. Methodological approaches for studying the microbial ecology of drinking water distribution systems. *Water Res.* 65, 134–156.
- Duan, S., Banger, K., Toor, G.S., 2021. Evidence of phosphate mining and Agriculture influence on Concentrations, forms, and ratios of nitrogen and phosphorus in a Florida River. *Water-Sui* 13, 1064.
- Emtiaz, F., Schwartz, T., Marten, S.M., Krolla-Sidenstein, P., Obst, U., 2004. Investigation of natural biofilms formed during the production of drinking water from surface water bankment filtration. *Water Res.* 38, 1197–1206.
- Eom, H., Borgatti, D., Paerl, H.W., Park, C., 2017. Formation of low-molecular-weight dissolved organic nitrogen in pre-denitrification biological nutrient removal systems and its impact on eutrophication in coastal waters. *Environ. Sci. Technol.* 51, 3776–3783.
- Feng, L., Xu, J., Kang, S., Li, X., Li, Y., Jiang, B., Shi, Q., 2016. Chemical composition of microbe-derived dissolved organic matter in cryoconite in Tibetan Plateau glaciers: insights from Fourier transform ion cyclotron resonance mass spectrometry analysis. *Environ. Sci. Technol.* 50, 13215–13223.
- Fill, J.M., Davis, C.N., Crandall, R.M., 2019. Climate change lengthens southeastern USA lightning-ignited fire seasons. *Glob Change Biol* 25, 3562–3569.
- Ganesh, S., Bertagnolli, A.D., Bristow, L.A., Padilla, C.C., Blackwood, N., Aldunate, M., et al., 2018. Single cell genomic and transcriptomic evidence for the use of alternative nitrogen substrates by anammox bacteria. *ISME J.* 12, 2706–2722.
- Gao, F., Zhang, H., Yang, F., Li, H., Zhang, R., 2014. The effects of zero-valent iron (ZVI) and ferrous iron (Fe<sup>2+</sup>) on anammox activity and granulation in an anaerobic continuously stirred tank reactors (CSTR). *Process Biochem.* 49, 1970–1978.
- Gibson, J.S., Harwood, C., 2002. Metabolic diversity in aromatic compound utilization by anaerobic microbes. *Annu. Rev. Microbiol.* 56, 345–369.
- Haga, H., Nagata, T., Sakamoto, M., 2001a. Ammonium regeneration within the euphotic zone. *Lake Kizaki: limnology and ecology of a Japanese lake*. Backhuys, Leiden 207–215.
- He, Z.Y., Sun, A., Jiao, X.Y., Ge, A.H., Hu, H.W., Jin, S., et al., 2022. Fertilization has a greater effect than rhizosphere on community structures of comammox nitrospira in an alkaline agricultural soil. *Appl. Soil Ecol.* 175, 104456.
- Hendrickson, C.L., Quinn, J.P., Kaiser, N.K., Smith, D.F., Blakney, G.T., Chen, T., et al., 2015. 21 Tesla Fourier transform ion cyclotron resonance mass spectrometer: a national resource for ultrahigh resolution mass analysis. *J. Am. Soc. Mass Spectrom.* 26, 1626–1632.
- Highton, M.P., Bakken, L.R., Dörsch, P., Wakelin, S., de Klein, C.A., Molstad, L., Morales, S.E., 2020. Soil N<sub>2</sub>O emission potential falls along a denitrification phenotype gradient linked to differences in microbiome, rainfall and carbon availability. *Soil Biol. Biochem.* 150, 108004.
- Hu, H., Ma, H., Ding, L., Geng, J., Xu, K., Huang, H., et al., 2016. Concentration, composition, bioavailability, and N-nitrosodimethylamine formation potential of particulate and dissolved organic nitrogen in wastewater effluents: a comparative study. *Sci. Total Environ.* 569, 1359–1368.
- Hu, Y., Li, N., Jiang, J., Xu, Y., Luo, X., Cao, J., 2022. Simultaneous Feammox and anammox process facilitated by activated carbon as an electron shuttle for autotrophic biological nitrogen removal. *Front. Environ. Sci. Eng.* 16, 1–13.
- Jackson, G.A., Williams, P.M., 1985. Importance of dissolved organic nitrogen and phosphorus to biological nutrient cycling. *Deep-Sea Res.* 32, 223–235.
- Jasinski, S.M., 2013. Mineral resource of the month: phosphate rock. *Earth*. 12.
- Jiang, X., Liu, C., Cai, J., Hu, Y., Shao, K., Tang, X., et al., 2023. Relationships between environmental factors and N-cycling microbes reveal the indirect effect of further eutrophication on denitrification and DNRA in shallow lakes. *Water Res.* 245, 120572.
- Jiang, X., Yao, L., Guo, L., Liu, G., Liu, W., 2017. Multi-scale factors affecting composition, diversity, and abundance of sediment denitrifying microorganisms in Yangtze lakes. *Appl Microbiol biot* 101, 8015–8027.
- Khan, E., Awobamise, M., Jones, K., Murthy, S., 2009. Method development for measuring biodegradable dissolved organic nitrogen in treated wastewater. *Water Environ. Res.* 81, 779–787.
- Koch, B.P., Kattner, G., Witt, M., Passow, U., 2014. Molecular insights into the microbial formation of marine dissolved organic matter: recalcitrant or labile? *Biogeosciences* 11, 4173–4190.
- Kujawinski, E.B., Del Vecchio, R., Blough, N.V., Klein, G.C., Marshall, A.G., 2004. Probing molecular-level transformations of dissolved organic matter: insights on photochemical degradation and protozoan modification of DOM from electrospray ionization Fourier transform ion cyclotron resonance mass spectrometry. *Mar. Chem.* 92, 23–37.
- Kuroda, K., Narihiro, T., Nobu, M.K., Tobo, A., Yamauchi, M., Yamada, M., 2021. Ecogenomics reveals microbial metabolic networks in a psychrophilic methanogenic bioreactor treating soy sauce production wastewater. *Microb. Environ.* 36, ME21045.
- Lapointe, B.E., Herren, L.W., Paule, A.L., 2017. Septic systems contribute to nutrient pollution and harmful algal blooms in the St. Lucie Estuary, Southeast Florida, USA. *Harmful Algae* 70, 1–22.
- Law, Y., Ye, L., Pan, Y., Yuan, Z., 2012. Nitrous oxide emissions from wastewater treatment processes. *Philos T Roy Soc B* 367, 1265–1277.
- Li, J., Zeng, W., Liu, H., Zhan, M., Miao, H., Hao, X., 2023. Achieving deep autotrophic nitrogen removal from low strength ammonia nitrogen wastewater in aeration sponge iron biofilter: simultaneous nitrification, Feammox, NDFO and Anammox. *Chem. Eng. J.* 460, 141755.
- Ling, J., Chen, S., 2005. Impact of organic carbon on nitrification performance of different biofilters. *Aquacult. Eng.* 33, 150–162.
- Liu, G., Wang, J., 2013. Long-term low DO enriches and shifts nitrifier community in activated sludge. *Environ. Sci. Technol.* 47, 5109–5117.
- Liu, H., Dong, Y., Liu, Y., Wang, H., 2010. Screening of novel low-cost adsorbents from agricultural residues to remove ammonia nitrogen from aqueous solution. *J. Hazard Mater.* 178, 1132–1136.
- Liu, H., Hu, H., Huang, X., Ge, T., Li, Y., Zhu, Z., et al., 2021a. Canonical ammonia oxidizers, rather than comammox Nitrospira, dominated autotrophic nitrification during the mineralization of organic substances in two paddy soils. *Soil Biol. Biochem.* 156, 108192.
- Liu, Q., Chen, Y., Xu, X.W., 2023a. Genomic insight into strategy, interaction and evolution of nitrifiers in metabolizing key labile-dissolved organic nitrogen in different environmental niches. *Front. Microbiol.* 14, 1273211.
- Liu, S., Dai, J., Wei, H., Li, S., Wang, P., Zhu, T., et al., 2021b. Dissimilatory nitrate reduction to ammonium (DNRA) and denitrification pathways are leveraged by cyclic AMP receptor protein (CRP) paralogs based on electron donor/acceptor limitation in *Shewanella loihica* PV-4. *Appl. Environ. Microbiol.* 87.
- Liu, Y., Xu, L., Su, J., Ali, A., Huang, T., Wang, Y., Zhang, P., 2023b. Microbially driven Fe-N cycle: intrinsic mechanisms, enhancement, and perspectives. *Sci. Total Environ.* 168084.
- Lusk, M.G., Toor, G.S., 2016. Biodegradability and molecular composition of dissolved organic nitrogen in urban stormwater runoff and outflow water from a stormwater retention pond. *Environ. Sci. Technol.* 50, 3391–3398.
- Ma, H., Gao, X., Chen, Y., Zhu, J., Liu, T., 2021. Fe (II) enhances simultaneous phosphorus removal and denitrification in heterotrophic denitrification by chemical precipitation and stimulating denitrifiers activity. *Environ. Pollut.* 287, 117668.
- Maria, S., Chattopadhyay, T., Ananya, S., Kundu, S., 2020. Reduction of nitrite to NO at a mononuclear copper (II)-phenolate site. *Inorg. Chim. Acta.* 506, 119515.
- Mohan, T.K., Nancharaiyah, Y.V., Venugopalan, V.P., Sai, P.S., 2016. Effect of C/N ratio on denitrification of high-strength nitrate wastewater in anoxic granular sludge sequencing batch reactors. *Ecol. Eng.* 91, 441–448.
- Mundinger, A.B., Lawson, C.E., Jetten, M.S., Koch, H., Lückner, S., 2019. Cultivation and transcriptional analysis of a canonical Nitrospira under stable growth conditions. *Front Microbiol* 10, 453054.
- Osborne, D.M., Podgorski, D.C., Bronk, D.A., Roberts, Q., Sipler, R.E., Austin, D., et al., 2013. Molecular-level characterization of reactive and refractory dissolved natural organic nitrogen compounds by atmospheric pressure photoionization coupled to Fourier transform ion cyclotron resonance mass spectrometry. *Rapid Commun. Mass Spectrom.* 27, 851–858.
- Palatinszky, M., Herbold, C., Jehmlich, N., Pogoda, M., Han, P., von Bergen, M., et al., 2015. Cyanate as an energy source for nitrifiers. *Nature* 524, 105–108.
- Pandey, C.B., Kumar, U., Kaviraj, M., Minick, K.J., Mishra, A.K., Singh, J.S., 2020. DNRA: a short-circuit in biological N-cycling to conserve nitrogen in terrestrial ecosystems. *Sci. Total Environ.* 738, 139710.
- Pehlivanoglu, E., Sedlak, D.L., 2004. Bioavailability of wastewater-derived organic nitrogen to the alga *Selenastrum capricornutum*. *Water Res.* 38, 3189–3196.
- Roots, P., Wang, Y., Rosenthal, A.F., Griffin, J.S., Sabba, F., Petrovich, M., et al., 2019. Comammox Nitrospira are the dominant ammonia oxidizers in a mainstream low dissolved oxygen nitrification reactor. *Water Res.* 157, 396–405.



- Rotthauwe, J.H., Witzel, K.P., Liesack, W., 1997. The ammonia monooxygenase structural gene *amoA* as a functional marker: molecular fine-scale analysis of natural ammonia-oxidizing populations. *Appl. Environ. Microbiol.* 63, 4704–4712.
- Shrestha, P., Hurley, S.E., Wemple, B.C., 2018. Effects of different soil media, vegetation, and hydrologic treatments on nutrient and sediment removal in roadside bioretention systems. *Ecol. Eng.* 112, 116–131.
- Simsek, H., Kasi, M., Ohm, J.B., Blonigen, M., Khan, E., 2013. Bioavailable and biodegradable dissolved organic nitrogen in activated sludge and trickling filter wastewater treatment plants. *Water Res.* 47, 3201–3210.
- Sinha, B., Annachatre, A.P., 2007. Partial nitrification—operational parameters and microorganisms involved. *Rev. Environ. Sci. Biotechnol.* 6, 285–313.
- Smith, D.F., Podgorski, D.C., Rodgers, R.P., Blakney, G.T., Hendrickson, C.L., 2018. 21 tesla FT-ICR mass spectrometer for ultrahigh-resolution analysis of complex organic mixtures. *Anal. Chem.* 90, 2041–2047.
- Snoeyenbos-West, O.L., Nevin, K.P., Anderson, R.T., Lovley, D.R., 2000. Enrichment of *Geobacter* species in response to stimulation of Fe (III) reduction in sandy aquifer sediments. *Microb. Ecol.* 39, 153–167.
- Sonthiphand, P., Neufeld, J.D., 2014. Nitrifying bacteria mediate aerobic ammonia oxidation and urea hydrolysis within the Grand River. *Aquat. Microb. Ecol.* 73, 151–162.
- Spang, A., Poehlein, A., Offre, P., Zumbrägel, S., Haider, S., Rychlik, N., et al., 2012. The genome of the ammonia-oxidizing *Candidatus Nitrososphaera gargensis*: insights into metabolic versatility and environmental adaptations. *Environ. Microbiol.* 14, 3122–3145.
- Stibal, M., Šabacká, M., Žárský, J., 2012. Biological processes on glacier and ice sheet surfaces. *Nat. Geosci.* 5, 771–774.
- Stults, J.R., Snoeyenbos-West, O., Methe, B., Lovley, D.R., Chandler, D.P., 2001. Application of the 5' fluorogenic exonuclease assay (TaqMan) for quantitative ribosomal DNA and rRNA analysis in sediments. *Appl. Environ. Microbiol.* 67, 2781–2789.
- Sun, H., Jiang, S., 2022. A review on nirS-type and nirK-type denitrifiers via a scientometric approach coupled with case studies. *Environ. Sci. Proc. Imp.* 24, 221–232.
- Sun, H., Shi, W., Cai, C., Ge, S., Ma, B., Li, X., Ding, J., 2020. Responses of microbial structures, functions, metabolic pathways and community interactions to different C/N ratios in aerobic nitrification. *Bioresour. Technol.* 311, 123422.
- Takahashi, M., 1981. Nitrogen metabolism in Lake Kizaki, Japan II. Distribution and decomposition of organic nitrogen. *Arch. Hydrobiol.* 92, 359–376.
- Tsushima, I., Kindaichi, T., Okabe, S., 2007. Quantification of anaerobic ammonium-oxidizing bacteria in enrichment cultures by real-time PCR. *Water Res.* 41, 785–794.
- van Spanning, R.J., Richardson, D.J., Ferguson, S.J., 2007. Introduction to the biochemistry and molecular biology of denitrification. In: *Biology of the Nitrogen Cycle*. Elsevier, pp. 3–20.
- Wang, H., Peng, L., Mao, N., Geng, J., Ren, H., Xu, K., 2021. Effects of Fe<sup>3+</sup> on microbial communities shifts, functional genes expression and nitrogen transformation during the start-up of Anammox process. *Bioresour. Technol.* 320, 124326.
- Watanabe, A., Tsutsuki, K., Inoue, Y., Maie, N., Melling, L., Jaffé, R., 2014. Composition of dissolved organic nitrogen in rivers associated with wetlands. *Sci. Total Environ.* 493, 220–228.
- Wetzel, R.G., 2001. *Limnology: Lake and River Ecosystems*. Gulf Professional Publishing.
- Wheeler, P.A., Kirchman, D.L., 1986. Utilization of inorganic and organic nitrogen by bacteria in marine systems I. *Limnol. Oceanogr.* 31, 998–1009.
- Xenopoulos, M.A., Barnes, R.T., Boodoo, K.S., Butman, D., Catalán, N., D'Amario, S.C., et al., 2021. How humans alter dissolved organic matter composition in freshwater: relevance for the Earth's biogeochemistry. *Biogeochemistry* 154, 323–348.
- Xia, F., Wang, J.G., Zhu, T., Zou, B., Rhee, S.K., Quan, Z.X., 2018. Ubiquity and diversity of complete ammonia oxidizers (comammox). *Appl. Environ. Microbiol.* 84.
- Xian, L., Zhang, Y., Cao, Y., Wan, T., Gong, Y., Dai, C., et al., 2020. Glutamate dehydrogenase plays an important role in ammonium detoxification by submerged macrophytes. *Sci. Total Environ.* 722, 137859.
- Xu, H., Lin, C., Shen, Z., Gao, L., Lin, T., Tao, H., et al., 2020a. Molecular characteristics of dissolved organic nitrogen and its interaction with microbial communities in a prechlorinated raw water distribution system. *Environ. Sci. Technol.* 54, 1484–1492.
- Xu, S., Wang, B., Li, Y., Jiang, D., Zhou, Y., Ding, A., et al., 2020b. Ubiquity, diversity, and activity of comammox *Nitrospira* in agricultural soils. *Sci. Total Environ.* 706, 135684.
- Xu, Y., Feng, L., Jeffrey, P.D., Shi, Y., Morel, F.M., 2008. Structure and metal exchange in the cadmium carbonic anhydrase of marine diatoms. *Nature* 452, 56–61.
- Ye, J., Zhao, S., Ren, J., Zhang, X., Xie, W., Meng, H., et al., 2024. Higher contribution by comammox bacteria than AOA and AOB to nitrification in the sediments of lake Taihu. *Int. Biodeterior. Biodegrad.* 187, 105709.
- Yin, G., Hou, L., Liu, M., Li, X., Zheng, Y., Gao, J., et al., 2017. DNRA in intertidal sediments of the Yangtze Estuary. *J. Geophys. Res.-Biogeosci.* 122, 1988–1998.
- Yoon, S., Cruz-García, C., Sanford, R., Ritalahti, K.M., Löffler, F.E., 2015. Denitrification versus respiratory ammonification: environmental controls of two competing dissimilatory NO<sub>3</sub><sup>-</sup>/NO<sub>2</sub><sup>-</sup> reduction pathways in *Shewanella loihica* strain PV-4. *ISME J.* 9, 1093–1104.
- Zehr, J.P., Paulsen, S.G., Axler, R.P., Goldman, C.R., 1988. Dynamics of dissolved organic nitrogen in subalpine Castle Lake, California. *Hydrobiologia* 157, 33–45.
- Zhang, Y.F., Zhang, C.H., Xu, J.H., Li, L., Li, D., Wu, Q., Ma, L.M., 2022. Strategies to enhance the reactivity of zero-valent iron for environmental remediation: a review. *J. Environ. Manag.* 317, 115381.
- Zheng, M., Mu, G., Zhang, A., Wang, J., Chang, F., Niu, J., et al., 2022. Predominance of comammox bacteria among ammonia oxidizers under low dissolved oxygen condition. *Chemosphere* 308, 136436.
- Zumft, W.G., 1997. Cell biology and molecular basis of denitrification. *Microbiol. Mol. Biol. Rev.* 61, 533–616.